

*Electronic Supplementary Information*

**Nitric Oxide Imaging in Cancer Enabled by Steric Relaxation of a Photoacoustic  
Probe Platform**

Christopher J. Reinhardt, Ruiwen Xu, Jefferson Chan\*

Department of Chemistry and the Beckman Institute for Advanced Science and Technology, University of Illinois at  
Urbana-Champaign, Urbana, IL, 61801

Correspondence should be addressed to J.C. (jeffchan@illinois.edu).

**Table of Contents.**

1. Materials	2
2. Instruments and Software	2
3. General Synthetic Procedures	3
4. Cell Culture	3
5. Computational Details	3
6. Photophysical Characterization	4
7. PA Imaging in Tissue-Mimicking Phantoms	4
8. Selectivity Studies	5
9. MTT Cytotoxicity Assay	5
10. PA Imaging of Exogenous NO in 4T1 Murine Breast Cancer Cells	5
11. Live Subject Statement	6
12. PA Imaging of LPS-induced Inflammation in BALB/c Mice	6
13. PA Imaging of 4T1 Murine Breast Cancer-Derived NO in BALB/c Mice	6
14. Synthetic Procedures	7
15. Supplemental Figures	16
16. NMR Spectroscopic Data	28
17. References	50

**Materials.** 3-(4,5-Dimethylthiazol-2-yl)-2,5-diphenyltetrazolium bromide (MTT reagent), and dichloromethane were purchased from Acros Organic. Nitromethane was purchased from Alfa Aesar. All deuterated solvents were purchased from Cambridge Isotope Laboratories. Diethylamine NONOate (DEA-NONOate) and methylamine hexamethylene methylamine NONOate (MAHMA-NONOate) was purchased from Cayman Chemicals. Tris(3-hydroxypropyltriazolylmethyl)amine was purchased from Click Chemistry Tools. Anhydrous ethanol (Decon Lab), ammonium chloride, chloroform, copper sulfate pentahydrate, Cremophor EL (CrEL, Fluka), diethyl ether, ethyl acetate, *n*-butanol, phosphate saline buffer (Corning), potassium phosphate dibasic, potassium phosphate monobasic, sodium bicarbonate, sodium chloride, and toluene were purchased from Fisher Scientific. Agarose LE (Molecular Biology Grade) was purchased from Gold Biotechnology. Acetonitrile, anhydrous methanol, concentrated hydrochloric acid, hydrogen peroxide (30 % v/v) and sodium hydroxide were purchased from Macron Fine Chemicals. Ammonium acetate, di-*tert*-butyl dicarbonate, diisopropylethylamine, ethylene dichloride, sodium ascorbate, methyl iodide, potassium carbonate, potassium hydroxide, potassium iodide, thophene-2-carbaldehydem, sodium azide, sodium sulfate (anhydrous), ferrous sulfate heptahydrate were purchased from Oakwood Chemicals. Anhydrous acetonitrile, anhydrous dichloromethane, anhydrous dimethylformamide, anhydrous dimethylsulfoxide, anhydrous tetrahydrofuran, boron trifluoride dietherate, celite 545, diethylamine (40 % w/w in water), hexanes, indocyanine green, iron(II) sulfate heptahydrate, iron(III) chloride (anhydrous), lipopolysaccharides from *Escherichia coli* O111:B4 (purified by phenol extraction), manganese(II) chloride, potassium permanganate, propargyl bromide (80 % w/w in toluene), sodium hydride (60 % dispersion in mineral oil), sodium ascorbate, L-N<sup>G</sup>-monomethyl-arginine acetate salt (L-NMMA), and sodium nitrite were purchased from Sigma Aldrich. Fluorinated ethylene propylene (FEP) tubing (wall thickness 0.01", inner diameters 0.08" and 0.12") was purchased from McMaster-Carr.

**Instruments and Software.** <sup>1</sup>H, <sup>13</sup>C, <sup>11</sup>B, and <sup>19</sup>F NMR spectra were acquired on Varian 400, Varian 500, or Carver B500 spectrometers. The following abbreviations were used to describe coupling constants: singlet (s), doublet (d), triplet (t), quartet (q), quintet (quint), multiplet (m), and broad singlet (bs). Spectra were visualized and analysed using MestReNova (version 10.0). High-resolution mass spectra were acquired with a Waters Q-TOF Ultima ESI mass spectrometer and a Waters Synapt G2-Si ESI/LC-MS mass spectrometer equipped with a PDA detector (200 – 500 nm). Ultraviolet–visible (UV–vis) measurements or spectra were recorded on a Cary 60 spectrometer or SpectraMax M2 plate reader (Molecular Devices). Fluorescence spectra were acquired on a QuantaMaster-400 scanning spectrofluorometer with micro fluorescence quartz cuvettes (Science Outlet). Refractive indices were measured using an RHB-32ATC Brix Refractometer. Photoacoustic imaging was performed using the Endra Nexus 128+ photoacoustic tomography system (Ann Arbor, MI, USA), and the data were analysed using Horos (version 3.0)

imaging software. All other data analysis was performed using Microsoft Excel or GraphPad Prism (version 6.0 or 8.0). A Mettler Toledo SevenCompact pH meter was used for pH measurements. All final figures were prepared in Adobe Illustrator (version 22.02.02).

**General Synthetic Procedures.** All materials were purchased from commercial vendors and used without further purification. Specific information regarding the material's sources can be found in the Supporting Information. Thin-layer chromatography (TLC) was performed on glass-backed TLC plates precoated with silica gel containing an UV254 fluorescent indicator (Macherey-Nagel). TLC's were visualized with a 254/365 nm UV hand-held amp (UVP). Flash silica gel chromatography was performed using 0.04 – 0.063 mm 60 M silica (Macherey-Nagel). Non-commercially available anhydrous solvents were dried over 4 Å molecular sieves activated via heating under a vacuum at 300 °C. All glassware used under anhydrous reaction conditions were flame-dried under vacuum and cooled immediately before use. When required, solutions were degassed by bubbling nitrogen through the solution for a minimum of 20 minutes. Saturated solutions of NO were generated by bubbling gaseous NO from the reaction between iron sulfate heptahydrate and sodium nitrite at 100 °C through the desired, degassed solvent (27 g iron sulfate heptahydrate and 12.5 g of sodium nitrite for ~2.5 L of NO).<sup>1</sup>

**Cell Culture.** 4T1 murine mammary carcinoma cells and 264.7 RAW macrophage cells were acquired from ATCC and Prof. Elvira de Mejia (Food Science and Human Nutrition, UIUC), respectively. Cells were cultured in phenol-red free RPMI 1640 medium or Dulbecco's modified eagle medium (DMEM, Corning) supplemented with 10 % fetal bovine serum (FBS, Sigma Aldrich), and 1 % penicillin/streptomycin (Corning). Cells were incubated at 37 °C with 5 % CO<sub>2</sub>. Cells were passaged using manual scraping (264.7 RAW macrophage cells) or trypsin (0.25% trypsin with 0.1% EDTA in HBSS without calcium, magnesium, and sodium bicarbonate, Corning, 4T1 murine mammary carcinoma cells) at least every 3 days.

**Computational Details.** Structures were built using Avagadro<sup>2</sup> and were optimized using the universal force field<sup>3</sup> until it converged. Further geometry optimizations were performed sequentially using density functional theory using Guassian 3. First, the structure was optimized using B3LYP<sup>4,5</sup> with the 6-31(d) basis set in the gas phase followed by B3LYP with the 6-31(d) basis set in implicit methanol solvent. All resulting structures were identified as a ground state by calculating the stretching frequencies. Dihedral angles were measured, using Chimera visualization software,<sup>6</sup> as the positive angle between the plane defined by all of the heavy atoms within the aza-BODIPY core and the plane defined by all heavy atoms in the ring of interest. Dihedral angles were reported as an average if the structure was

symmetrical. UV-Vis spectra were calculated from the solvent optimized structure using time-dependent self-consistent frequencies density functional theory using the CAM-B3LYP functional<sup>7</sup> and 6-31(d) basis set for only singlet excitations in an implicit methanol solvent.

**Photophysical Characterization.** Extinction coefficients and fluorescence quantum yields were acquired in experimental triplicates. *N*-nitrosated products were generated by reacting SR-APNO with NO (150 equiv. from MAHMA-NONOate solution in ethanolic 20 mM potassium phosphate buffer, pH 7.4, 50% v/v or 60 equiv. in methanol, generated from ~15 mM saturated methanolic solution) for greater than 1 h at room temperature, where complete conversion was confirmed via UV-vis spectroscopy. Extinction coefficients were acquired by titrating the compound into methanol (final DMSO concentration < 1%) within the linear range (typically absorbance values between 0.05 and 1.50) or from the absorbance of a solution of known concentration. Fluorescence quantum yields were obtained using a modified method for relative fluorescence quantum yield.<sup>8</sup> Samples were prepared in ethanolic 20 mM potassium phosphate buffer (pH 7.4, 50% v/v, final DMSO concentration < 1%) and sequentially diluted ( $n = 4$ ) while monitoring both absorbance and fluorescence. Absorbance was kept low (< 0.1) to prevent secondary absorbance events. Relative quantum yields were calculated relative to dimethoxy aza-BODIPY ( $\phi = 0.36$ , chloroform)<sup>9</sup> with refractive indexes of 1.445 and 1.3573 for chloroform and ethanolic 20 mM potassium phosphate buffer (pH 7.4, 50% v/v), respectively.<sup>10</sup> All samples were excited at 640 nm and emission was monitored from 660 – 890 nm with a slit width of 2.0 nm.

**PA Imaging in Tissue-Mimicking Phantoms.** Tissue phantoms were prepared from agarose (4 g) in a solution of 2% reduced fat milk (2 mL) and deionized water (78 mL). The mixture was heated in a microwave oven until a viscous gel was produced (30 s); followed by an additional 15 – 30 s of heating to ensure homogeneity. The gel was allowed to cool in a custom Teflon mould that fits within the Endra Nexus 128+ bowl system with hypodermal steel tubing inserted to prepare channels for placing FEP tubes (0.08-inch diameter) containing the samples. The tissue-mimicking phantom was allowed to set for greater than 1 h at 4 °C before use. Sample solutions (200  $\mu$ L) were pipetted into FEP tubing (0.08-inch diameter) and sealed by folding over the ends and securing with a short length of 0.12-inch diameter FEP tubing. SR-APNO (25  $\mu$ M for theoretical maximum ratiometric comparisons; 10  $\mu$ M for PA spectra) was dissolved in an ethanolic 20 mM potassium phosphate buffer (pH 7.4, 50% v/v). *t*-SR-APNO was generated by reacting SR-APNO with NO (500 equiv. NO from MAHMA-NONOate) for greater than 1 h at room temperature (complete conversion was confirmed by UV-vis). Images were acquired using continuous mode with 6 second rotation time. PA spectra were measured in the same solvent at 10 nm intervals, and signal was integrated

over the total range of signal. Mean signals are reported as the average of the two samples and the experiment was performed in experimental triplicate.

**Selectivity Studies.** The initial absorbance (300 – 1000 nm) and fluorescence (excitation at 688 nm; emission collected between 698 and 898 nm) were measured before the addition of 200 equiv. reactive metals, oxygen, nitrogen, and carbonyl species (unless otherwise noted). After addition, the reaction was sealed and incubated at room temperature for 1 h. Final measurements were recorded, and relative turn-on was determined by the sum of intensity over the total range of emission. Fe(II) selectivity studies were performed in ethanolic 20 mM HEPES buffer (pH 7.4, 50% v/v) to prevent oxidation. All metal solutions were prepared in water from their chloride salt, except for Fe(II) which was prepared from  $\text{FeSO}_4 \cdot (\text{H}_2\text{O})_7$ . Aqueous formaldehyde solutions were depolymerized by heating to solution to 100 °C for greater than 15 min before use. Aqueous dehydroascorbic acid solutions were prepared by heating at 60 °C for greater than 15 min before use. Aqueous perchlorate, nitrite, and nitrate solutions were prepared for their corresponding sodium salts. Superoxide anion was added as a solution of potassium superoxide in DMSO. Nitroxyl was generated *in situ* from a solution of Angeli's salt in degassed 10 mM potassium hydroxide solution. NO was generated *in situ* from a solution of MAHMA-NONOate in degassed 10 mM potassium hydroxide. Hydroxyl radical was generated via Fenton chemistry between Mohr's salt (solution in degassed 1 M aqueous hydrochloric acid) and hydrogen peroxide. Fe(II), nitroxyl, and hydroxyl radical selectivity assays were performed under nitrogen to prevent oxidation. Peroxynitrite was synthesized according to a literature report.<sup>11</sup> All other analytes were prepared by dilution from commercially available sources.

**MTT Cytotoxicity Assay.** A 96-well plate was seeded with 20,000 cells per well (200  $\mu\text{L}$  of 100,000 cells/mL) and incubated at 37 °C with 5 %  $\text{CO}_2$  for 24 h (~70 % confluent). Media was removed and fresh serum-free RPMI 1640 containing vehicle control (DMSO) or SR-APNO for a final concentration of 1, 5, or 15  $\mu\text{M}$  (1.25 % DMSO v/v). After 8 or 24 h the media was removed and replaced with 200  $\mu\text{L}$  20:1 mixture of FBS-free RMPA 1640 and (3-(4,5-dimethylthiazol-2-yl)-2,5-diphenyl-tetrazolium bromide (MTT, 5 mg/mL stock in PBS). The cells were incubated for 4 h under the same conditions and then the medium was removed and replaced with DMSO (100  $\mu\text{L}$ /well). The absorbance of each well was recorded at 555 nm on a microplate reader. Viability was calculated by the absorbance relative to the vehicle control.

**PA Imaging of Exogenous NO in 4T1 Murine Breast Cancer Cells.** A T75 flask of 4T1 murine mammary carcinoma cells was seeded and allowed to grow to confluency (~90%) over 36 h. The cells were trypsinized,

suspended in a 15  $\mu\text{M}$  solution of SR-APNO-3 (RMPA 1640 serum-free media with 0.75% DMSO final concentration) and  $2 \times 10^6$  cells were distributed into each 1.6 mL Eppendorf tube. The cells were stained for 1 h at 37 °C with agitation. After staining, the cells were collected via centrifugation (6,000 rpm, 5 min, 4 °C), washed with PBS (1 mL, same protocol as collection) to remove free dye, and then resuspended in PBS (450  $\mu\text{L}$ ). Samples were treated with control (50  $\mu\text{L}$  10 mM KOH), 1 mM DEA-NONOate (50  $\mu\text{L}$  10 mM DEA-NONOate in 10 mM KOH), or 5 mM DEA-NONOate (50  $\mu\text{L}$  50 mM DEA-NONOate in 10 mM KOH) and were allowed to incubate with rocking for 2 h at room temperature. The cells were pelleted via centrifugation (6,000 rpm, 5 min, 4 °C) and imaged directly in the 1.6 mL Eppendorf tube. Images were acquired at the appropriate wavelengths (SR-APNO-3: 790 nm; t-SR-APNO-3: 690 nm) using continuous mode with a 6 s rotation time. Quantification of each cell pellet is reported as the average of the mean signals over the entire area of interest (12.1 mm, slices 130 – 256).

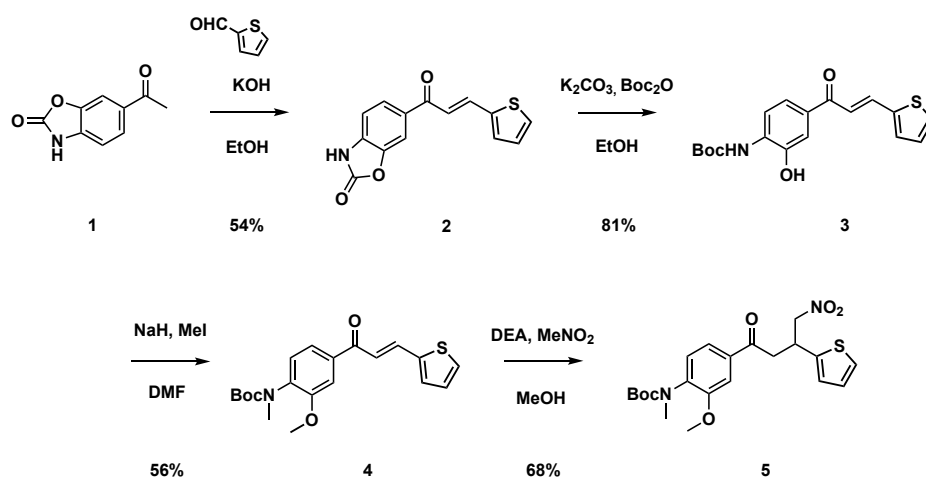
**Live-Subject Statement.** All animal experiments were performed with the approval of the Institutional Animal Care and Use Committee of the University of Illinois at Urbana–Champaign, following the principles outlined by the American Physiological Society on research animal use.

**PA Imaging of LPS-induced Inflammation in BALB/c Mice.** Six to eight-week-old BALB/c mice were obtained from Jackson Laboratory and intramuscularly administered lipopolysaccharide in a saline solution (4 mg/kg). After 4 h, APNO-5 or SR-APNO-3 (50  $\mu\text{M}$ , 25  $\mu\text{L}$ ) was administered intramuscularly in a sterile saline solution (0.9% NaCl in sterile water) containing 15% DMF (v/v). Inhibition assays were performed by preparing the aforementioned dye solution in sterile saline containing 35 mM L-NMMA for co-administration. Images were acquired in technical replicates ( $n = 2$ ) at the appropriate wavelengths using continuous mode with a 6 s rotation time. Quantification of each image is reported as the average of the mean signals of the technical replicates over the entire area of interest (12.1 mm, slices 130 – 256). For more clear representation, images corresponding to the probe and N-nitrosated products were coloured independently and then overlaid using Horos software.

**PA Imaging of 4T1 Murine Breast Cancer-Derived NO in BALB/c Mice.** Six to eight-week-old BALB/c mice were obtained from Jackson Laboratory and 4T1 subcutaneous tumours ( $5 \times 10^4$  cells, 50  $\mu\text{L}$  of  $1 \times 10^6$  cells/mL in 1:1 serum-free RPMI 1640 media and Matrigel) were implanted and allowed to grow for 26 days for a final volume of ~300-400  $\text{mm}^3$ . Tumour volumes were measured using a calliper method<sup>12</sup> and the body weight was monitored over the course of the experiment. SR-APNO-3 (50  $\mu\text{M}$ , 25  $\mu\text{L}$ ) was administered intratumorally or subcutaneously in a sterile saline solution (0.9% NaCl in sterile water) containing 15% DMF (v/v). Inhibition assays were performed by

preparing the aforementioned dye solution in sterile saline containing 35 mM L-NMMA for co-administration. Images were acquired in technical replicates ( $n = 2$ ) using continuous mode with a 6 s rotation time. Quantification of each image is reported as the average of the mean signals of the technical replicates over the entire area of interest (12.1 mm, slices 130 – 256). Reported samples sizes correspond to the number of biological replicates (animals). For more clear representation, images corresponding to the probe and N-nitrosated products were coloured independently and then overlaid using Horos software.

### Synthetic Procedures.



**Scheme 1.** Synthesis of compound 5.

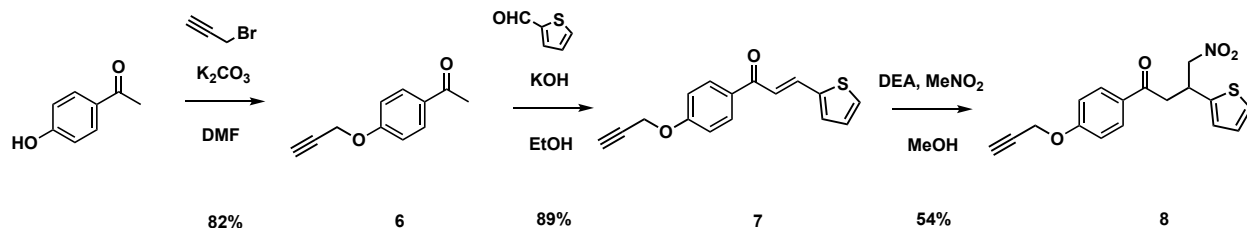
**6-Acetylbenzo[d]oxazol-2(3H)-one (1).** The compound was prepared according to previously reported procedures.<sup>10,13</sup>

**(E)-6-(3-(thiophen-2-yl)acryloyl)benzo[d]oxazol-2(3H)-one (2).** A solution of **1** (3.49 g, 19.7 mmol, 1.0 equiv.) and 2-thiophenecarboxaldehyde (2.03 mL, 21.7 mmol, 1.1 equiv.) in EtOH (100.0 mL) was treated with dropwise addition of aq. KOH (10 M, 5.92 mL, 59.2 mmol, 3.0 equiv.). The reaction was allowed to stir at room temperature for 12 h. After completion, the mixture was concentrated and purified via silica gel column chromatography (1% MeOH/CH<sub>2</sub>Cl<sub>2</sub>) to afford the product as a yellow solid (2.88 g, 10.6 mmol, 54% yield).  $R_f = 0.09$  (25% Acetone/Hexanes). <sup>1</sup>H NMR (500 MHz, DMSO-*d*<sub>6</sub>)  $\delta$  12.06 (s, 1H), 8.01 (d,  $J = 1.5$  Hz, 1H), 7.99 (dd,  $J = 8.1, 1.7$  Hz, 1H), 7.90 (d,  $J = 15.2$  Hz, 1H), 7.78 (d,  $J = 4.9$  Hz, 1H), 7.69 – 7.68 (m, 1H), 7.60 (d,  $J = 15.2$  Hz, 1H), 7.22 (d,  $J = 8.1$  Hz, 1H), 7.19 (dd,  $J = 5.0, 3.6$  Hz, 1H). <sup>13</sup>C NMR (125 MHz, DMSO-*d*<sub>6</sub>)  $\delta$  187.30, 154.89, 143.94, 140.23, 136.90, 135.35, 133.12, 132.24, 130.87, 129.14, 126.05, 120.59, 109.97, 109.80. HRMS (ESI, TOF) calc'd for [M+H]<sup>+</sup> 272.0381, found 272.0387.

**tert-butyl (E)-(2-hydroxy-4-(3-(thiophen-2-yl)acryloyl)phenyl)carbamate (3).** A solution of **2** (2.63 g, 9.69 mmol, 1.0 equiv.), K<sub>2</sub>CO<sub>3</sub> (4.01 g, 29.0 mmol, 3.0 equiv.), di-*tert*-butyl dicarbonate (8.50 g, 38.9 mmol, 4.0 equiv.) in MeOH (50.0 mL) was heated to 45 °C for 7 h. The reaction was quenched with sat. ammonium chloride and then the product extracted with EtOAc (3×). The organic layers were combined, dried over anhydrous Na<sub>2</sub>SO<sub>4</sub>, concentrated, and purified via silica gel column chromatography (30% EtOAc/Hexanes with 0.1% AcOH) to afford the product as a yellow solid (2.69 g, 7.80 mmol, 81% yield). R<sub>f</sub> = 0.28 (30% EtOAc/Hexanes). <sup>1</sup>H NMR (500 MHz, CDCl<sub>3</sub>) δ 8.34 (s, 1H), 7.94 (d, *J* = 15.2 Hz, 1H), 7.85 (d, *J* = 1.9 Hz, 1H), 7.81 (d, *J* = 8.4 Hz, 1H), 7.59 (dd, *J* = 8.4, 1.8 Hz, 1H), 7.43 (d, *J* = 5.1 Hz, 1H), 7.21 (s, 1H), 7.12 – 7.07 (m, 1H), 1.55 (s, 9H). <sup>13</sup>C NMR (125 MHz, CDCl<sub>3</sub>) δ 189.02, 153.29, 145.69, 140.43, 137.21, 133.04, 132.14, 131.80, 128.99, 128.36, 122.31, 120.40, 118.43, 116.35, 81.79, 28.28. HRMS (ESI, TOF) calc'd for [M+H]<sup>+</sup> 346.1113, found 346.1119.

**tert-butyl (E)-(2-methoxy-4-(3-(thiophen-2-yl)acryloyl)phenyl)(methyl)carbamate (4).** A pressure flask was charged with **2** (2.63 g, 7.62 mmol, 1.0 equiv.), anhydrous DMF (38.0 mL), methyl iodide (2.43 mL, 38.2 mmol, 5.0 equiv.), and NaH (60 wt %, 9.18 mg, 23.0 mmol, 3.0 equiv.) at 0 °C. The reaction was allowed to warm to room temperature and stirred for 1 h before heating to 70 °C for 12 h. The reaction cooled to room temperature and then was diluted in brine. The product was extracted with EtOAc (3×), the organic layers were combined, dried over anhydrous Na<sub>2</sub>SO<sub>4</sub>, concentrated and purified via silica gel column chromatography (25% EtOAc/Hexanes) to afford the product as a yellow solid (1.60 g, 4.30 mmol, 56% yield). R<sub>f</sub> = 0.13 (10% EtOAc/Hexanes). <sup>1</sup>H NMR (500 MHz, CDCl<sub>3</sub>) δ 7.94 (d, *J* = 15.3 Hz, 1H), 7.58 – 7.54 (m, 2H), 7.43 – 7.39 (m, 1H), 7.36 (d, *J* = 3.6 Hz, 1H), 7.31 (d, *J* = 15.3 Hz, 1H), 7.28 – 7.24 (m, 1H), 7.08 (dd, *J* = 5.1, 3.6 Hz, 1H), 3.91 (s, 3H), 3.15 (s, 3H), 1.39 (s, 9H). <sup>13</sup>C NMR (125 MHz, CDCl<sub>3</sub>) δ 188.96, 155.29, 155.05, 140.46, 137.67, 137.34, 137.14, 132.20, 128.98, 128.49, 121.25, 120.66, 111.29, 80.15, 55.78, 36.87, 28.35. HRMS (ESI, TOF) calc'd for [M+H]<sup>+</sup> 374.1426, found 374.1432.

**tert-butyl (2-methoxy-4-(4-nitro-3-(thiophen-2-yl)butanoyl)phenyl)(methyl)carbamate (5).** A solution of **3** (1.00 g, 2.68 mmol, 1.0 equiv.), nitromethane (0.72 mL, 13.0 mmol, 5.0 equiv.), and diethylamine (0.83 mL, 8.10 mmol, 3.0 equiv.) in MeOH (30.0 mL) was heated to 65 °C for 14 h. The reaction was concentrated and purified via silica gel column chromatography (30% EtOAc/Hexanes) to afford the product as a yellow solid (0.62 g, 2.68 mmol, 53% yield). R<sub>f</sub> = 0.34 (30% EtOAc/Hexanes). <sup>1</sup>H NMR (500 MHz, CDCl<sub>3</sub>) δ 7.46 (d, *J* = 7.4 Hz, 2H), 7.19 (d, *J* = 8.0 Hz, 1H), 7.13 (d, *J* = 5.1 Hz, 1H), 6.91 (d, *J* = 3.4 Hz, 1H), 6.86 (t, *J* = 4.4 Hz, 1H), 4.78 (dd, *J* = 12.7, 6.3 Hz, 1H), 4.66 (dd, *J* = 12.8, 7.8 Hz, 1H), 4.49 (p, *J* = 6.9 Hz, 1H), 3.82 (s, 3H), 3.45 (qd, *J* = 17.7, 6.7 Hz, 2H), 3.09 (s, 3H), 1.34 (s, 9H). <sup>13</sup>C NMR (125 MHz, CDCl<sub>3</sub>) δ 195.63, 155.05, 154.67, 141.87, 137.66, 135.57, 128.56, 127.06, 125.45, 124.61, 120.95, 110.56, 80.02, 79.80, 55.55, 42.23, 36.64, 34.77, 28.15. HRMS (ESI, TOF) calc'd for [M+H]<sup>+</sup> 435.1590, found 435.1601.

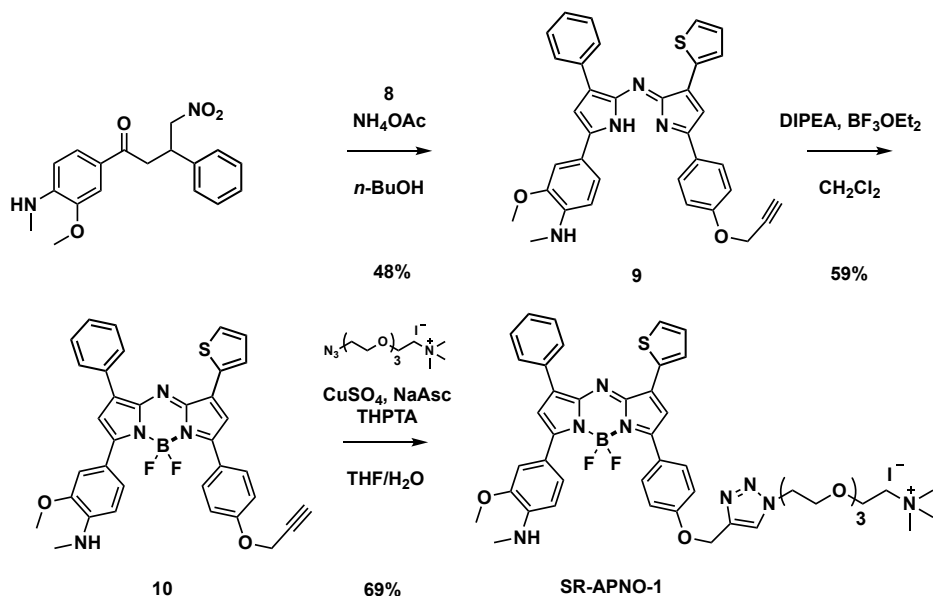


**Scheme 2.** Synthesis of compound **8**.

**1-(4-(prop-2-yn-1-yloxy)phenyl)ethan-1-one (6).** A suspension of 1-(4-hydroxyphenyl)ethan-1-one (575 mg, 4.23 mmol, 1.0 equiv.),  $K_2CO_3$  (759 mg, 5.49 mmol, 1.3 equiv.) in anhydrous DMF (10.0 mL) was treated with 3-bromoprop-1-yne (0.52 mL, 5.49 mmol, 1.3 equiv.) and heated to 65 °C for 1 h. The reaction was added with water and filtered by vacuum to afford the product as a pale yellow solid (603 mg, 4.23 mmol, 82% yield).  $R_f = 0.24$  (10% EtOAc/Hexanes).  $^1H$  NMR (500 MHz,  $CDCl_3$ )  $\delta$  7.86 (d,  $J = 9.0$  Hz, 2H), 6.64 (d,  $J = 9.1$  Hz, 2H), 3.04 (s, 6H), 2.50 (s, 3H).  $^{13}C$  NMR (125 MHz,  $CDCl_3$ )  $\delta$  196.36, 153.39, 130.51, 125.36, 110.60, 40.02, 25.98. HRMS (ESI, TOF) calc'd for  $[M+H]^+$  175.0759, found 175.0764.

**(E)-1-(4-(prop-2-yn-1-yloxy)phenyl)-3-(thiophen-2-yl)prop-2-en-1-one (7).** A solution of **6** (1.69 g, 9.72 mmol, 1.0 equiv.) and thiophene-2-carbaldehyde (1.0 mL, 11.0 mmol, 1.2 equiv.) in EtOH (50.0 mL) was treated dropwise with an aq. solution of KOH (10 M, 2.90 mL, 29.2 mmol, 3.0 equiv.). The reaction was allowed to stir at room temperature for 1 h before the resulting yellow precipitate was collected via filtration to afford the product as a yellow solid (2.32 g, 9.72 mmol, 89% yield).  $R_f = 0.26$  (10% EtOAc/Hexanes).  $^1H$  NMR (500 MHz,  $CDCl_3$ )  $\delta$  8.03 (d,  $J = 8.6$  Hz, 2H), 7.93 (d,  $J = 15.3$  Hz, 1H), 7.40 (d,  $J = 5.0$  Hz, 1H), 7.36 – 7.30 (m, 2H), 7.10 – 7.04 (m, 3H), 4.77 (d,  $J = 2.4$  Hz, 2H), 2.56 (t,  $J = 2.4$  Hz, 1H).  $^{13}C$  NMR (125 MHz,  $CDCl_3$ )  $\delta$  188.10, 161.22, 140.54, 136.62, 131.85, 131.78, 130.64, 128.55, 128.33, 120.59, 114.74, 77.82, 76.18, 55.89. HRMS (ESI, TOF) calc'd for  $[M+H]^+$  269.0636, found 269.0623.

**4-nitro-1-(4-(prop-2-yn-1-yloxy)phenyl)-3-(thiophen-2-yl)butan-1-one (8).** A solution of **7** (3.41 g, 12.7 mmol, 1.0 equiv.), nitromethane (3.44 mL, 63.6 mmol, 5.0 equiv.), and diethylamine (4.0 mL, 38.17 mmol, 3.0 equiv.) in MeOH (130.0 mL) was heated to 65 °C for 14 h. The reaction was concentrated and purified via silica gel column chromatography (20% EtOAc/Hexanes) to afford the product as a yellow solid (2.30 g, 6.98 mmol, 54% yield).  $R_f = 0.27$  (20% EtOAc/Hexanes).  $^1H$  NMR (500 MHz,  $CDCl_3$ )  $\delta$  7.95 – 7.92 (m, 2H), 7.21 (dt,  $J = 5.0, 1.2$  Hz, 1H), 7.04 – 7.01 (m, 2H), 6.97 – 6.93 (m, 2H), 4.87 – 4.82 (m, 1H), 4.76 (dd,  $J = 2.4, 1.0$  Hz, 2H), 4.70 (ddd,  $J = 12.6, 7.6, 1.0$  Hz, 1H), 3.52 – 3.40 (m, 2H), 2.55 (t,  $J = 2.4$  Hz, 1H), 2.17 (s, 1H), 1.54 (s, 1H).  $^{13}C$  NMR (125 MHz,  $CDCl_3$ )  $\delta$  206.89, 194.85, 161.71, 142.01, 130.31, 130.06, 127.12, 125.53, 124.66, 114.81, 79.92, 76.28, 55.89, 41.97, 34.86, 30.91. HRMS (ESI, TOF) calc'd for  $[M+H]^+$  330.0800, found 330.0790.



**Scheme 3.** Synthesis of **SR-APNO-1**.

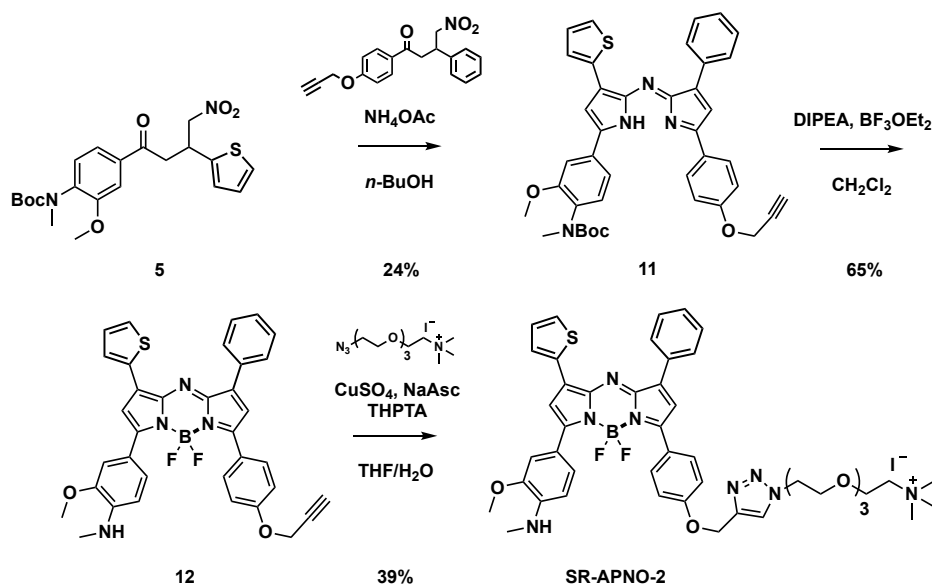
**1-(3-methoxy-4-(methylamino)phenyl)-4-nitro-3-phenylbutan-1-one.** The compound was prepared according to previously reported procedures.<sup>10</sup>

**tert-butyl (Z)-(2-methoxy-4-(4-phenyl-5-((5-(4-(prop-2-yn-1-yloxy)phenyl)-3-(thiophen-2-yl)-2H-pyrrol-2-ylidene)amino)-1H-pyrrol-2-yl)phenyl)(methyl)carbamate (9).** A suspension of 1-(3-methoxy-4-(methylamino)phenyl)-4-nitro-3-phenylbutan-1-one (267.7 mg, 815.2  $\mu\text{mol}$ , 1.0 equiv.), and **8** (805.5 mg, 2.45 mmol, 3.0 equiv.) in *n*-butanol (16.0 mL) was heated to 110 °C to dissolve all solids.  $\text{NH}_4\text{OAc}$  (942.6 mg, 12.23 mmol, 15 equiv.) was added in a single portion and the reaction was stirred at the same temperature for 5 h. Volatiles were removed under reduced pressure, the residue was suspended in brine, and the product was extracted with  $\text{CH}_2\text{Cl}_2$  (3 $\times$ ). The combined organic layers were dried over anhydrous  $\text{Na}_2\text{SO}_4$ , concentrated, and purified via silica gel column chromatography (90%  $\text{CH}_2\text{Cl}_2$ /Hexanes) to afford the product as blue solid (219.8 mg, 0.82 mmol, 48% yield).  $R_f = 0.32$  (50%  $\text{CH}_2\text{Cl}_2$ /Hexanes)  $^1\text{H NMR}$  (500 MHz,  $\text{CDCl}_3$ )  $\delta$  8.12 – 8.09 (m, 2H), 7.77 – 7.73 (m, 2H), 7.65 (dd,  $J = 3.6, 1.2$  Hz, 1H), 7.58 (dd,  $J = 8.2, 1.8$  Hz, 1H), 7.55 (d,  $J = 1.8$  Hz, 1H), 7.47 (dd,  $J = 8.2, 7.0$  Hz, 2H), 7.41 – 7.36 (m, 1H), 7.33 (dd,  $J = 5.0, 1.1$  Hz, 1H), 7.08 (dd,  $J = 5.1, 3.6$  Hz, 1H), 7.02 – 6.98 (m, 2H), 6.88 (s, 1H), 6.64 (d,  $J = 8.3$  Hz, 1H), 4.93 – 4.85 (m, 1H), 4.75 (d,  $J = 2.4$  Hz, 2H), 4.03 (s, 3H), 3.01 – 2.95 (m, 3H), 2.58 (t,  $J = 2.3$  Hz, 1H).  $^{13}\text{C NMR}$  (125 MHz,  $\text{CDCl}_3$ )  $\delta$  163.62, 158.13, 156.09, 146.95, 146.30, 144.15, 143.13, 142.90, 136.97, 133.80, 131.23, 129.68, 128.31, 128.24, 127.40, 126.81, 126.35, 125.87, 125.77, 123.86, 120.70, 119.05, 115.50, 108.47, 108.21, 106.97, 78.37, 76.08, 56.08, 55.47, 30.02, 29.85. HRMS (ESI, TOF) calc'd for  $[\text{M}+\text{H}]^+$  569.1987, found 569.1994.

**4-(5,5-difluoro-1-phenyl-7-(4-(prop-2-yn-1-yloxy)phenyl)-9-(thiophen-2-yl)-5H-5λ4,6λ4-dipyrrolo[1,2-c:2',1'-f][1,3,5,2]triazaborinin-3-yl)-2-methoxy-N-methylaniline (10).** A solution of **9** (97.2 mg, 0.17 mmol, 1.0 equiv.) and *N,N*-diisopropylethylamine (0.45 mL, 2.56 mmol, 15.0 equiv.) in anhydrous CH<sub>2</sub>Cl<sub>2</sub> (8.5 mL) was treated with boron trifluoride diethyl etherate (0.33 mL, 2.56 mmol, 15.0 equiv.). The reaction was allowed to stir at room temperature for 3 h under a nitrogen atmosphere. After completion, the reaction was quenched with minimal sat. aq. NaHCO<sub>3</sub> and diluted in brine. The product was extracted with CH<sub>2</sub>Cl<sub>2</sub> (3×), the combined organic layers were dried over anhydrous Na<sub>2</sub>SO<sub>4</sub>, concentrated, and purified via silica gel column chromatography (80% CH<sub>2</sub>Cl<sub>2</sub>/Hexanes) to afford the product as a purple solid (62.3 mg, 0.10 mmol, 59% yield). *R*<sub>f</sub> = 0.31 (50% CH<sub>2</sub>Cl<sub>2</sub>/Hexanes) <sup>1</sup>H NMR (500 MHz, CDCl<sub>3</sub>) δ 8.15 – 8.12 (m, 2H), 8.05 – 8.02 (m, 2H), 7.96 (d, *J* = 1.9 Hz, 1H), 7.78 (dd, *J* = 8.5, 2.0 Hz, 1H), 7.69 (dd, *J* = 3.7, 1.1 Hz, 1H), 7.53 – 7.49 (m, 2H), 7.47 – 7.43 (m, 2H), 7.25 (s, 1H), 7.12 (dd, *J* = 5.1, 3.7 Hz, 1H), 7.04 (d, *J* = 9.0 Hz, 2H), 6.83 (s, 1H), 6.63 (d, *J* = 8.6 Hz, 1H), 4.76 (d, *J* = 2.4 Hz, 2H), 3.94 (s, 3H), 2.99 (d, *J* = 5.3 Hz, 3H), 2.56 (t, *J* = 2.4 Hz, 1H). <sup>13</sup>C NMR (125 MHz, CDCl<sub>3</sub>) δ 160.44, 158.84, 152.94, 146.38, 143.81, 143.14, 135.83, 132.45, 131.03, 129.77, 129.41, 128.66, 128.60, 128.38, 127.77, 127.48, 127.38, 126.23, 125.49, 120.29, 118.54, 115.64, 114.76, 114.46, 110.94, 108.47, 78.43, 75.96, 55.98, 55.80, 31.74, 29.81, 22.81, 14.27. <sup>19</sup>F NMR (471 MHz, CDCl<sub>3</sub>) δ -131.18 (dd, *J* = 65.4, 32.5 Hz). <sup>11</sup>B NMR (161 MHz, CDCl<sub>3</sub>) δ 1.28 (t, *J* = 32.7 Hz). HRMS (ESI, TOF) calc'd for [M+H]<sup>+</sup> 616.1916, found 616.1988.

**SR-APNO-1.** A solution of **10** (18.2 mg, 28.8 μmol, 1.0 equiv.), 3,3',3''-((nitriлотris(methylene))tris(1H-1,2,3-triazole-4,1-diy))tris(propan-1-ol) (4.50 mg, 10.4 μmol, 0.4 equiv.), 2-(2-(2-(2-azidoethoxy)ethoxy)ethoxy)-N,N,N-trimethylethan-1-aminium iodide (38.3 mg, 98.5 μmol, 3.4 equiv.), and copper(II) sulfate pentahydrate (36.0 mg, 144.1 μmol, 5.0 equiv.), in anhydrous THF (6.0 mL) was treated with dropwise sodium ascorbate (8.6 mg, 43.2 μmol, 1.5 equiv.) in water (0.7 mL, degassed) at room temperature for 3 h under nitrogen atmosphere. The volatiles were removed by reduced pressure and the residual was diluted in 50% MeOH/CH<sub>2</sub>Cl<sub>2</sub> and washed with sat. aq. sodium iodide (2×). The combined organic layers were dried over anhydrous Na<sub>2</sub>SO<sub>4</sub>, concentrated, and purified via silica gel column chromatography (10% MeOH/CHCl<sub>3</sub>) to afford the product as a purple solid (20.3 mg, 19.9 μmol, 69% yield). *R*<sub>f</sub> = 0.22 (10% MeOH/CHCl<sub>3</sub>). <sup>1</sup>H NMR (500 MHz, CD<sub>2</sub>Cl<sub>2</sub>) δ 8.18 – 8.13 (m, 2H), 8.08 – 8.02 (m, 1H), 7.91 (s, 1H), 7.83 (dd, *J* = 8.6, 2.0 Hz, 1H), 7.71 (dd, *J* = 3.7, 1.2 Hz, 1H), 7.54 (dd, *J* = 8.2, 6.7 Hz, 2H), 7.50 – 7.45 (m, 2H), 7.32 (s, 1H), 7.17 – 7.10 (m, 3H), 6.90 (s, 1H), 6.68 (s, 0H), 5.29 (s, 2H), 4.62 – 4.52 (m, 2H), 3.96 (s, 3H), 3.90 (q, *J* = 4.9, 4.4 Hz, 2H), 3.75 (dq, *J* = 7.5, 2.7 Hz, 2H), 3.64 – 3.50 (m, 7H), 3.42 – 3.35 (m, 2H), 3.04 (s, 8H), 3.00 (d, *J* = 4.8 Hz, 3H). <sup>13</sup>C NMR (125 MHz, CD<sub>2</sub>Cl<sub>2</sub>) δ 160.25, 159.50, 146.85, 146.23, 144.14, 143.60, 135.30, 133.31, 132.02, 130.88, 129.57, 129.50, 128.84, 128.62, 127.71, 127.61, 127.49, 125.65, 124.45, 120.52, 117.92, 114.73, 114.08, 110.65, 108.37, 70.49, 70.39, 70.22, 70.11, 69.30, 66.23, 64.87, 61.80, 55.86, 55.04, 55.01, 54.98, 50.55, 29.69. <sup>19</sup>F NMR

(471 MHz, CD<sub>2</sub>Cl<sub>2</sub>) δ -130.30 (dd, *J* = 65.4, 32.3 Hz). <sup>11</sup>B NMR (161 MHz, CD<sub>2</sub>Cl<sub>2</sub>) δ 1.27 (t, *J* = 32.9 Hz). HRMS (ESI, TOF) calc'd for [M]<sup>+</sup> 877.3837, found 877.3842.



Scheme 4. Synthesis of SR-APNO-2.

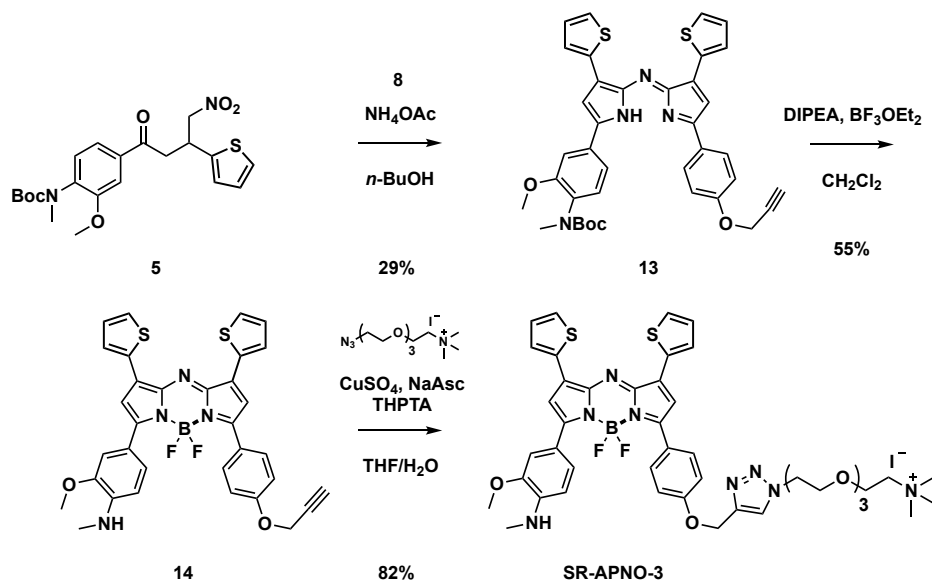
**tert-butyl (Z)-(2-methoxy-4-(5-((3-phenyl-5-(4-(prop-2-yn-1-yloxy)phenyl)-2H-pyrrol-2-ylidene)amino)-4-(thiophen-2-yl)-1H-pyrrol-2-yl)phenyl)(methyl)carbamate (11).** A suspension of 4-nitro-3-phenyl-1-(4-(prop-2-yn-1-yloxy)phenyl)butan-1-one (415.5 mg, 956.2 μmol, 1.0 equiv.), and **5** (947.6 mg, 2.93 mmol, 3.1 equiv.) in *n*-butanol (19.0 mL) was heated to 110 °C to dissolve all solids. NH<sub>4</sub>OAc (1.106 g, 14.34 mmol, 15 equiv.) was added in a single portion and reaction was stirred at the same temperature for 6 h. Volatiles were removed under reduced pressure, the residue was suspended in brine, and the product was extracted with CH<sub>2</sub>Cl<sub>2</sub> (3×). The combined organic layers were dried over anhydrous Na<sub>2</sub>SO<sub>4</sub>, concentrated, and purified via silica gel column chromatography (90% CH<sub>2</sub>Cl<sub>2</sub>/Hexanes) to afford the product as a blue solid (131.2 mg, 0.96 mmol, 24% yield). *R*<sub>f</sub> = 0.48 (100% CH<sub>2</sub>Cl<sub>2</sub>) <sup>1</sup>H NMR (500 MHz, CDCl<sub>3</sub>) δ 8.08 – 8.05 (m, 2H), 7.94 – 7.91 (m, 2H), 7.73 – 7.71 (m, 1H), 7.47 (dd, *J* = 8.4, 6.9 Hz, 2H), 7.44 (d, *J* = 7.5 Hz, 2H), 7.41 – 7.37 (m, 2H), 7.15 (s, 1H), 7.10 (dd, *J* = 5.1, 3.7 Hz, 1H), 7.09 – 7.03 (m, 2H), 4.79 (d, *J* = 2.4 Hz, 2H), 4.01 (s, 3H), 3.20 (s, 3H), 2.60 – 2.58 (m, 1H), 1.43 (s, 9H). <sup>13</sup>C NMR (125 MHz, CDCl<sub>3</sub>) δ 159.46, 158.78, 155.30, 155.24, 144.06, 136.07, 135.74, 133.57, 131.55, 129.52, 128.32, 128.28, 128.20, 127.50, 127.33, 126.98, 125.84, 119.20, 115.83, 115.49, 111.77, 108.61, 80.01, 77.98, 76.17, 55.97, 55.42, 47.43, 29.72, 28.34, 14.14. HRMS (ESI, TOF) calc'd for [M+H]<sup>+</sup> 668.2457, found 669.2540.

**4-(5,5-difluoro-9-phenyl-7-(4-(prop-2-yn-1-yloxy)phenyl)-1-(thiophen-2-yl)-5H-5λ4,6λ4-dipyrrolo[1,2-c:2',1'-f][1,3,5,2]triazaborinin-3-yl)-2-methoxy-*N*-methylaniline (12).** A solution of **11** (183.6 mg, 0.32 mmol, 1.0 equiv.)

and *N,N*-diisopropylethylamine (0.84 mL, 4.84 mmol, 15 equiv.) in anhydrous CH<sub>2</sub>Cl<sub>2</sub> (16.0 mL) was treated with boron trifluoride diethyl etherate (0.62 mL, 4.84 mmol, 15 equiv.). The reaction was stirred at room temperature for 6 h under a nitrogen atmosphere and then was quenched with minimal sat. aq. NaHCO<sub>3</sub>. The solution was then diluted with brine and the product was extracted with CH<sub>2</sub>Cl<sub>2</sub> (3×). The combined organic layers were dried over anhydrous Na<sub>2</sub>SO<sub>4</sub>, concentrated, and purified via silica gel column chromatography (80% CH<sub>2</sub>Cl<sub>2</sub>/Hexanes) to afford the product as a purple solid (128.7 mg, 0.32 mmol, 65% yield). *R*<sub>f</sub> = 0.36 (50% CH<sub>2</sub>Cl<sub>2</sub>/Hexanes) <sup>1</sup>H NMR (500 MHz, CDCl<sub>3</sub>) δ 8.11 – 8.08 (m, 2H), 8.07 – 8.04 (m, 2H), 7.93 (s, 1H), 7.83 (dd, *J* = 3.7, 1.1 Hz, 1H), 7.75 (dd, *J* = 8.5, 2.0 Hz, 1H), 7.52 (dd, *J* = 5.0, 1.1 Hz, 1H), 7.48 (t, *J* = 7.7 Hz, 2H), 7.39 (td, *J* = 7.1, 1.3 Hz, 1H), 7.17 – 7.12 (m, 2H), 7.06 – 7.02 (m, 2H), 6.92 (s, 1H), 6.61 (d, *J* = 8.5 Hz, 1H), 5.10 (s, 1H), 4.76 (d, *J* = 2.4 Hz, 2H), 3.93 (s, 3H), 2.97 (s, 3H), 2.56 (t, *J* = 2.4 Hz, 1H). <sup>13</sup>C NMR (125 MHz, CDCl<sub>3</sub>) δ 160.88, 158.67, 152.43, 146.39, 146.20, 143.66, 143.25, 139.16, 138.02, 134.41, 133.42, 130.97, 129.91, 129.34, 128.89, 128.46, 128.29, 127.82, 127.08, 126.32, 118.22, 116.99, 116.86, 114.62, 110.71, 108.30, 78.31, 75.83, 55.84, 55.66, 31.61, 29.66, 22.67, 14.14. <sup>19</sup>F NMR (471 MHz, CDCl<sub>3</sub>) δ -131.08 (dd, *J* = 65.3, 32.4 Hz). <sup>11</sup>B NMR (161 MHz, CDCl<sub>3</sub>) δ 1.29 (t, *J* = 32.7 Hz). HRMS (ESI, TOF) calc'd for [M+H]<sup>+</sup> 569.1987, found 569.1994.

**SR-APNO-2.** A solution of **12** (28.2 mg, 44.7 μmol, 1.0 equiv.), 3,3',3''-((nitriлотris(methylene))tris(1H-1,2,3-triazole-4,1-diy))tris(propan-1-ol) (5.60 mg, 12.9 μmol, 0.3 equiv.), 2-(2-(2-(2-azidoethoxy)ethoxy)ethoxy)-*N,N,N*-trimethylethan-1-aminium iodide (57.2 mg, 147 μmol, 3.3 equiv.), and copper(II) sulfate pentahydrate (55.7 mg, 223 μmol, 5.0 equiv.), in anhydrous THF (8.9 mL) was treated with dropwise sodium ascorbate (46.2 mg, 233.0 μmol, 5.2 equiv.) in water (1.1 mL, degassed) at room temperature under nitrogen atmosphere. The reaction was allowed to stir at the same temperature for 2 h before heating to 65 °C for an additional 4 h. The volatiles were removed by reduced pressure, the reaction was diluted in 50% MeOH/DCM, and the organic layer was washed with sat. aq. sodium iodide (2×). The combined organic layers were dried over anhydrous Na<sub>2</sub>SO<sub>4</sub>, concentrated, and purified via silica gel column chromatography (10% MeOH/CHCl<sub>3</sub>) to afford the product as a purple solid (17.6 mg, 17.3 μmol, 39% yield). *R*<sub>f</sub> = 0.25 (10% MeOH/CHCl<sub>3</sub>). <sup>1</sup>H NMR (500 MHz, CD<sub>2</sub>Cl<sub>2</sub>) δ 8.14 – 8.10 (m, 2H), 8.07 (d, *J* = 8.4 Hz, 2H), 7.94 (bs, 1H), 7.89 (d, *J* = 1.9 Hz, 1H), 7.86 (dd, *J* = 3.8, 1.1 Hz, 1H), 7.81 (dd, *J* = 8.5, 2.0 Hz, 1H), 7.60 (dd, *J* = 5.0, 1.1 Hz, 1H), 7.51 (t, *J* = 7.6 Hz, 2H), 7.44 – 7.39 (m, 1H), 7.23 (s, 1H), 7.19 (dd, *J* = 5.1, 3.7 Hz, 1H), 7.14 (d, *J* = 8.5 Hz, 2H), 6.98 (s, 1H), 6.67 (d, *J* = 8.5 Hz, 1H), 4.57 (t, *J* = 4.9 Hz, 2H), 3.97 (s, 3H), 3.91 (t, *J* = 4.9 Hz, 2H), 3.74 (dt, *J* = 6.8, 3.0 Hz, 2H), 3.62 – 3.58 (m, 2H), 3.54 (m, 6H), 3.39 – 3.35 (m, 2H), 3.05 (s, 9H), 3.01 (s, 3H). <sup>13</sup>C NMR (126 MHz, CD<sub>2</sub>Cl<sub>2</sub>) δ 160.87, 159.46, 151.66, 146.37, 146.21, 144.09, 142.95, 138.84, 133.98, 133.18, 130.98, 130.52, 129.23, 129.13, 128.56, 128.46, 127.92, 127.32, 125.88, 117.77, 117.19, 116.67, 114.72, 110.56, 108.31, 70.56, 70.36, 70.30, 70.17, 69.19, 66.20, 64.86, 61.84, 55.85, 55.00, 54.97, 54.95, 50.62, 31.93, 29.68, 22.69, 13.87. <sup>19</sup>F NMR

(471 MHz, CD<sub>2</sub>Cl<sub>2</sub>) δ -130.31 (dd, *J* = 60.0, 27.5 Hz). <sup>11</sup>B NMR (161 MHz, CD<sub>2</sub>Cl<sub>2</sub>) δ 1.27 (t, *J* = 32.8 Hz). HRMS (ESI, TOF) calc'd for [M]<sup>+</sup> 877.3845, found 877.3844.



**Scheme 5: Synthesis of SR-APNO-3.**

**tert-butyl (Z)-(2-methoxy-4-(5-(5-(4-(prop-2-yn-1-yloxy)phenyl)-3-(thiophen-2-yl)-2H-pyrrol-2-ylidene)amino)-4-(thiophen-2-yl)-1H-pyrrol-2-yl)phenyl(methyl)carbamate (13).** A suspension of **5** (0.24 g, 0.55 mmol, 1.0 equiv.), and **8** (0.49 g, 1.50 mmol, 2.7 equiv.) in *n*-butanol (11.0 mL) was heated to 110 °C to dissolve all solids. NH<sub>4</sub>OAc (0.84 g, 11.0 mmol, 20 equiv.) was added in a single portion and reaction was stirred at the same temperature for 6 h. Volatiles were removed under reduced pressure, the resulting solid was suspended in brine, and the product was extracted with CH<sub>2</sub>Cl<sub>2</sub> (3×). The combined organic layers were dried over anhydrous Na<sub>2</sub>SO<sub>4</sub>, concentrated, and purified via silica gel column chromatography (step gradient: 90% CH<sub>2</sub>Cl<sub>2</sub>/Hexanes, 100% CH<sub>2</sub>Cl<sub>2</sub>, then 1% MeOH/CH<sub>2</sub>Cl<sub>2</sub>) to afford the product as a blue solid (0.11 g, 0.55 mmol, 29% yield). *R*<sub>f</sub> = 0.63 (100 % CH<sub>2</sub>Cl<sub>2</sub>) <sup>1</sup>H NMR (500 MHz, DMSO-*d*<sub>6</sub>) δ 12.77 (s, 1H), 8.17 – 8.12 (m, 2H), 7.97 (d, *J* = 3.6 Hz, 1H), 7.90 – 7.86 (m, 1H), 7.76 (d, *J* = 5.0 Hz, 1H), 7.72 (d, *J* = 5.0 Hz, 1H), 7.64 (d, *J* = 1.8 Hz, 1H), 7.62 – 7.57 (m, 2H), 7.52 (s, 1H), 7.40 (d, *J* = 8.1 Hz, 1H), 7.24 (ddd, *J* = 6.8, 5.0, 3.6 Hz, 2H), 7.17 (d, *J* = 8.8 Hz, 2H), 4.97 (d, *J* = 2.4 Hz, 2H), 4.06 (s, 3H), 3.69 (t, *J* = 2.3 Hz, 1H), 3.11 (s, 3H), 1.37 (s, 9H). <sup>13</sup>C NMR (125 MHz, DMSO-*d*<sub>6</sub>) δ 159.77, 159.49, 154.86, 154.07, 151.63, 149.52, 145.08, 138.12, 135.19, 134.78, 133.70, 133.64, 130.32, 129.07, 128.98, 128.27, 128.24, 127.95, 127.82, 127.41, 126.89, 124.69, 118.87, 115.67, 115.56, 112.14, 108.82, 79.12, 78.80, 78.76, 55.78, 55.49, 55.45, 27.90. HRMS (ESI, TOF) calc'd for [M+H]<sup>+</sup> 675.2100, found 675.2103.

**4-(5,5-difluoro-7-(4-(prop-2-yn-1-yloxy)phenyl)-1,9-di(thiophen-2-yl)-5H-5λ<sup>4</sup>,6λ<sup>4</sup>-dipyrrolo[1,2-c:2',1'-**

**f][1,3,5,2]triazaborinin-3-yl)-2-methoxy-N-methylaniline (14).** A solution of **13** (0.24 g, 0.35 mmol, 1.0 equiv.) and *N,N*-diisopropylethylamine (0.92 mL, 5.20 mmol, 15 equiv.) in anhydrous CH<sub>2</sub>Cl<sub>2</sub> (15.0 mL) was treated with boron trifluoride diethyl etherate (0.67 mL, 5.20 mmol, 15 equiv.). The reaction was stirred at room temperature for 3 h under a nitrogen atmosphere. The reaction was quenched with minimal sat. aq. NaHCO<sub>3</sub> and then extracted with CH<sub>2</sub>Cl<sub>2</sub> (3×) from brine. The combined organic layers were dried over anhydrous Na<sub>2</sub>SO<sub>4</sub>, concentrated, and purified via silica gel column chromatography (step gradient: 20% CH<sub>2</sub>Cl<sub>2</sub>/Hexanes to 60% CH<sub>2</sub>Cl<sub>2</sub>/Hexanes, 10% steps) to afford the product as a purple solid (0.12 g, 0.19 mmol, 55% yield). R<sub>f</sub> = 0.25 (50% CH<sub>2</sub>Cl<sub>2</sub>/Hexanes) <sup>1</sup>H NMR (500 MHz, CD<sub>2</sub>Cl<sub>2</sub>) δ 8.04 (d, *J* = 2.1 Hz, 1H), 8.02 (d, *J* = 3.0 Hz, 2H), 7.91 (d, *J* = 1.9 Hz, 1H), 7.85 – 7.79 (m, 2H), 7.60 (dd, *J* = 5.0, 1.2 Hz, 1H), 7.51 (dd, *J* = 5.1, 1.1 Hz, 1H), 7.25 – 7.21 (m, 2H), 7.19 (dd, *J* = 5.1, 3.6 Hz, 1H), 7.08 – 7.03 (m, 2H), 6.88 (s, 1H), 6.66 (d, *J* = 8.6 Hz, 1H), 5.27 (q, *J* = 5.5 Hz, 1H), 4.79 (d, *J* = 2.4 Hz, 2H), 3.94 (s, 3H), 2.99 (d, *J* = 5.0 Hz, 3H), 2.63 (t, *J* = 2.3 Hz, 1H). <sup>13</sup>C NMR (125 MHz, CD<sub>2</sub>Cl<sub>2</sub>) δ 161.22, 159.27, 152.39, 146.97, 146.83, 144.74, 142.99, 138.35, 136.15, 134.81, 133.42, 131.40, 131.36, 130.38, 130.09, 128.82, 128.70, 128.45, 128.30, 128.05, 126.61, 118.36, 115.14, 111.23, 108.83, 78.85, 76.14, 56.43, 56.24, 30.26, 30.07. <sup>19</sup>F NMR (471 MHz, CD<sub>2</sub>Cl<sub>2</sub>) δ -130.74 (dd, *J* = 65.4, 32.6 Hz). <sup>11</sup>B NMR (161 MHz, CD<sub>2</sub>Cl<sub>2</sub>) δ 1.22 (t, *J* = 32.7 Hz). HRMS (ESI, TOF) calc'd for [M+H]<sup>+</sup> 623.1558, found 623.1568.

**SR-APNO-3.** A solution of **14** (23.8 mg, 38.0 μmol, 1.0 equiv.), 3,3',3''-((nitriлотris(methylene))tris(1H-1,2,3-triazole-4,1-diy))tris(propan-1-ol) (3.15 mg, 7.25 μmol, 0.2 equiv.), 2-(2-(2-(2-azidoethoxy)ethoxy)ethoxy)-*N,N,N*-trimethylethan-1-aminium iodide (44.0 mg, 114 μmol, 2.97 equiv.), copper(II) sulfate pentahydrate (96.1 mg, 385 μmol, 10 equiv.), and anhydrous THF (1.9 mL) was treated dropwise with a solution of sodium ascorbate (15.8 mg, 79.8 μmol, 2.1 equiv.) in water (382 μL, degassed). The reaction was then heated to 65 °C for 3 h under nitrogen atmosphere. The volatiles were removed under reduced pressure, the residue was diluted in 50% MeOH/CH<sub>2</sub>Cl<sub>2</sub>, and the organic layer was washed with sat. aq. sodium iodide (2×). The organic layer was collected, dried over anhydrous Na<sub>2</sub>SO<sub>4</sub>, concentrated, and purified via silica gel column chromatography (5 % MeOH/CHCl<sub>3</sub>) to afford the product as a purple solid (31.8 mg, 31.5 μmol, 82% yield). R<sub>f</sub> = 0.09 (5% MeOH/CHCl<sub>3</sub>). <sup>1</sup>H NMR (500 MHz, DMSO-*d*<sub>6</sub>) δ 8.33 (s, 1H), 8.26 (s, 1H), 8.15 (d, *J* = 3.7 Hz, 1H), 8.13 – 8.08 (m, 1H), 8.05 (d, *J* = 8.5 Hz, 2H), 7.98 – 7.87 (m, 4H), 7.74 (d, *J* = 5.0 Hz, 1H), 7.34 – 7.29 (m, 1H), 7.25 – 7.22 (m, 1H), 7.22 – 7.15 (m, 4H), 6.74 (d, *J* = 8.9 Hz, 1H), 5.26 (s, 2H), 4.57 (t, *J* = 5.2 Hz, 2H), 3.94 (s, 3H), 3.84 (t, *J* = 5.3 Hz, 2H), 3.82 – 3.77 (m, 2H), 3.57 – 3.46 (m, 12H), 3.32 (s, 3H), 3.08 (s, 9H), 2.93 (d, *J* = 5.1 Hz, 3H). <sup>13</sup>C NMR (125 MHz, DMSO-*d*<sub>6</sub>) δ 159.89, 158.99, 148.74, 146.10, 146.02, 145.41, 142.34, 140.59, 136.89, 134.90, 133.06, 131.53, 130.40, 130.16, 130.01, 129.52, 128.95, 128.21, 127.99, 127.55, 125.03, 119.35, 116.01, 114.60, 114.12, 110.84,

109.01, 79.20, 69.56, 69.52, 69.40, 69.32, 68.67, 64.39, 64.02, 61.23, 55.62, 53.07, 53.04, 49.45, 29.33, 18.55.  $^{19}\text{F}$  NMR (471 MHz,  $\text{DMSO-}d_6$ )  $\delta$  -129.11 (dd,  $J = 66.4, 29.7$  Hz).  $^{11}\text{B}$  NMR (161 MHz,  $\text{DMSO-}d_6$ )  $\delta$  1.26 (t,  $J = 33.1$  Hz). HRMS (ESI, TOF) calc'd for  $[\text{M}]^+$  883.3047, found 883.3395.

### Supplemental Figures.

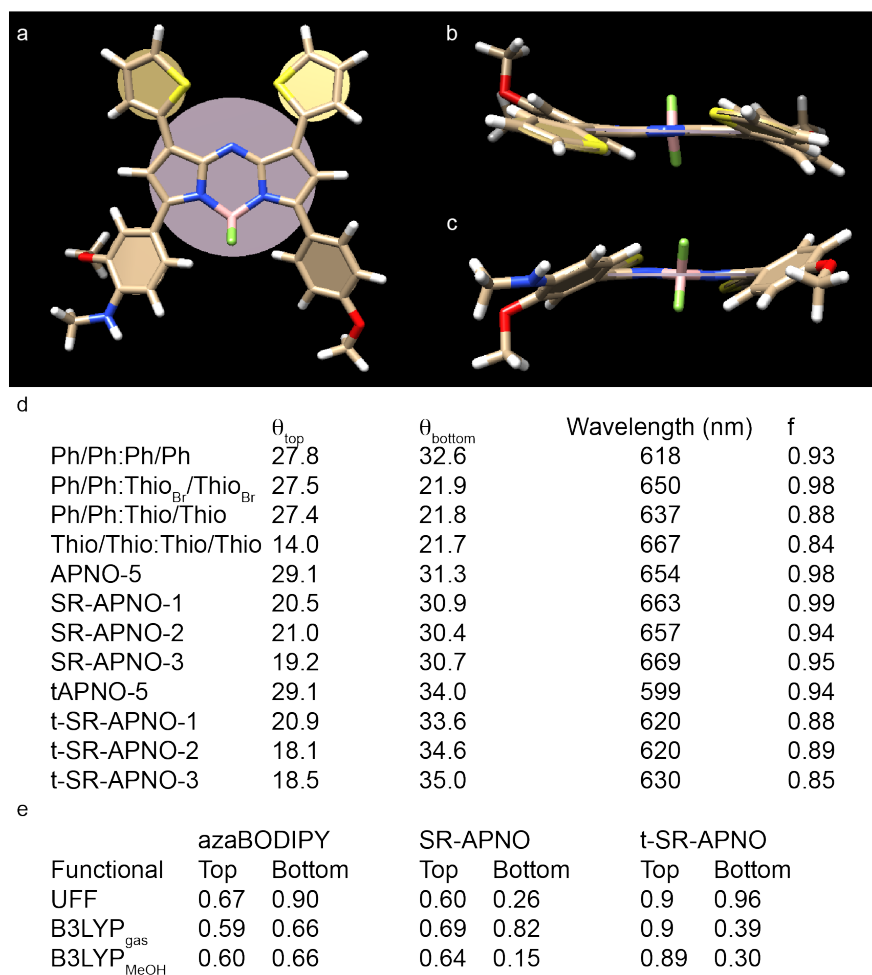


**Figure S1.** (a-c) Representative structure and definition of planes for the aza-BODIPY and SR-aza-BODIPY platforms. Planes corresponding to the phenyl (Ph), thiophene (Thio), and aza-BODIPY core are defined by all heavy atoms in the plane. Dihedral angle is calculated between each ring and the core and reported as the average of the absolute values. (d) Tabulated average dihedral angles from reported X-ray crystallographic data (names defined as top-left/top-right: bottom-left/bottom-right: Ph/Ph:Ph/Ph, Ph/Ph:Thio-Br/Thio-Br, Ph/Ph:Thio/Thio, and Thio/Thio:Thio/Thio),<sup>14,15</sup> APNO-5, and SR-APNO series after geometry optimization using B3LYP in implicit methanol with the corresponding time-dependent DFT calculation of absorption maxima with CAM B3LYP in implicit methanol. (e) Linear regressions for measured calculated absorbance maximum versus dihedral angle. Note that poor correlation between the bottom dihedral angles and calculated absorption maxima was because this was not sampled with the structures.

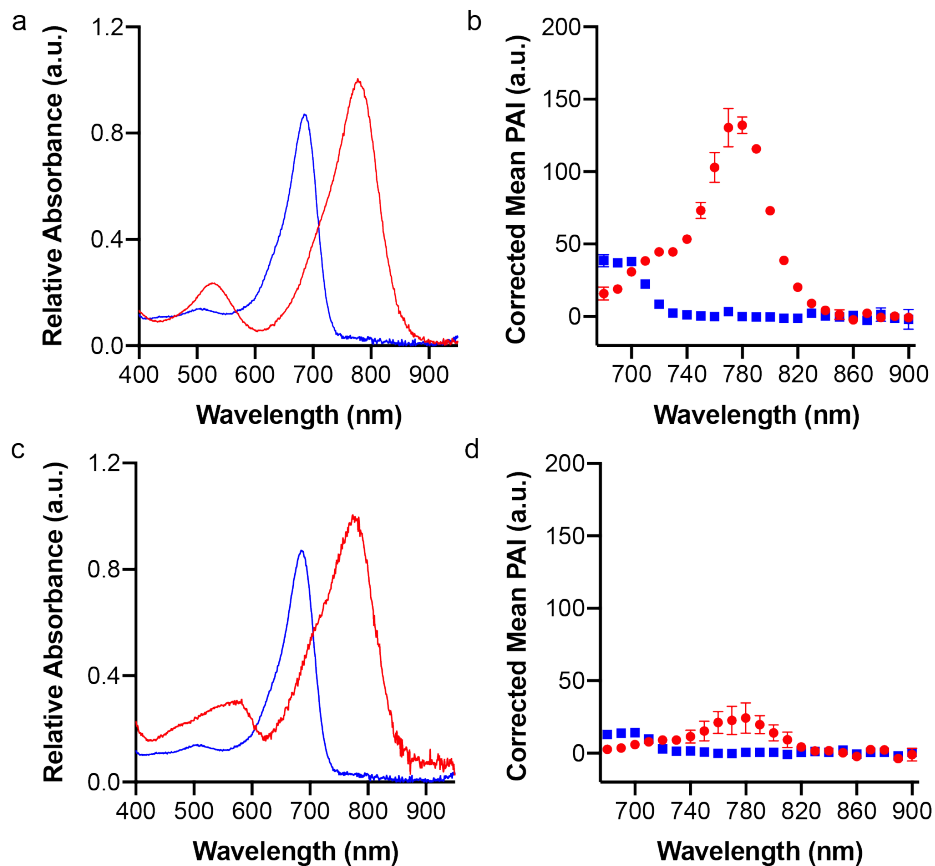


**Figure S2.** UV-Vis (2  $\mu\text{M}$ ) and PA spectra (10  $\mu\text{M}$ ) for (a-b) SR-APNO-1 and (c-d) SR-APNO-2 in ethanolic 20 mM potassium phosphate buffer (pH 7.4, 50% v/v). Data is reported as the mean  $\pm$  standard deviation ( $n = 3$ ).

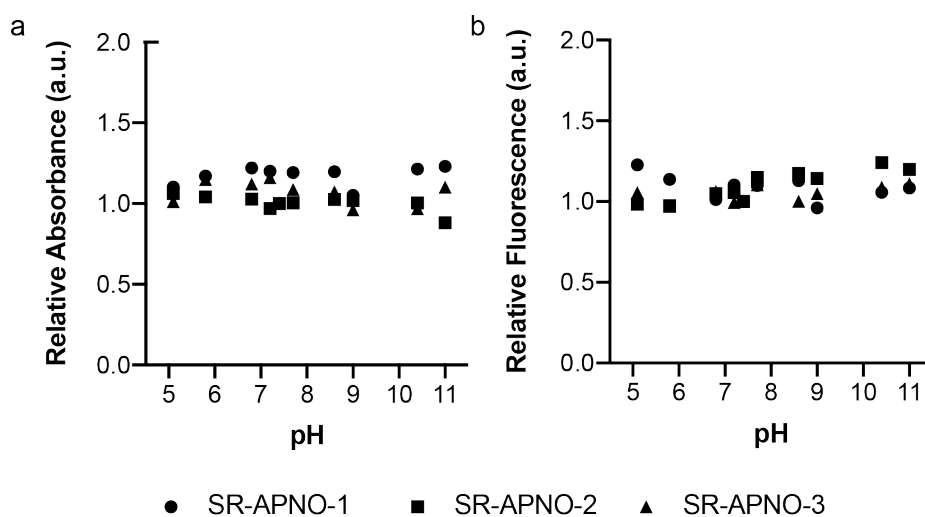


**Figure S3.** The effect of pH on SR-APNO (2.5  $\mu\text{M}$ ) (a) absorbance (350 – 950 nm) and (b) fluorescence (excitation at 650 nm, emission collected from 660-950 nm) properties in ethanolic 20 mM Britton-Robinson buffer (50 % v/v).<sup>16,17</sup> Relative absorbance and fluorescence are calculated relative to the absorption maxima and sum fluorescence intensity at pH 7.4. No changes were observed in either the absorption or emission spectra.

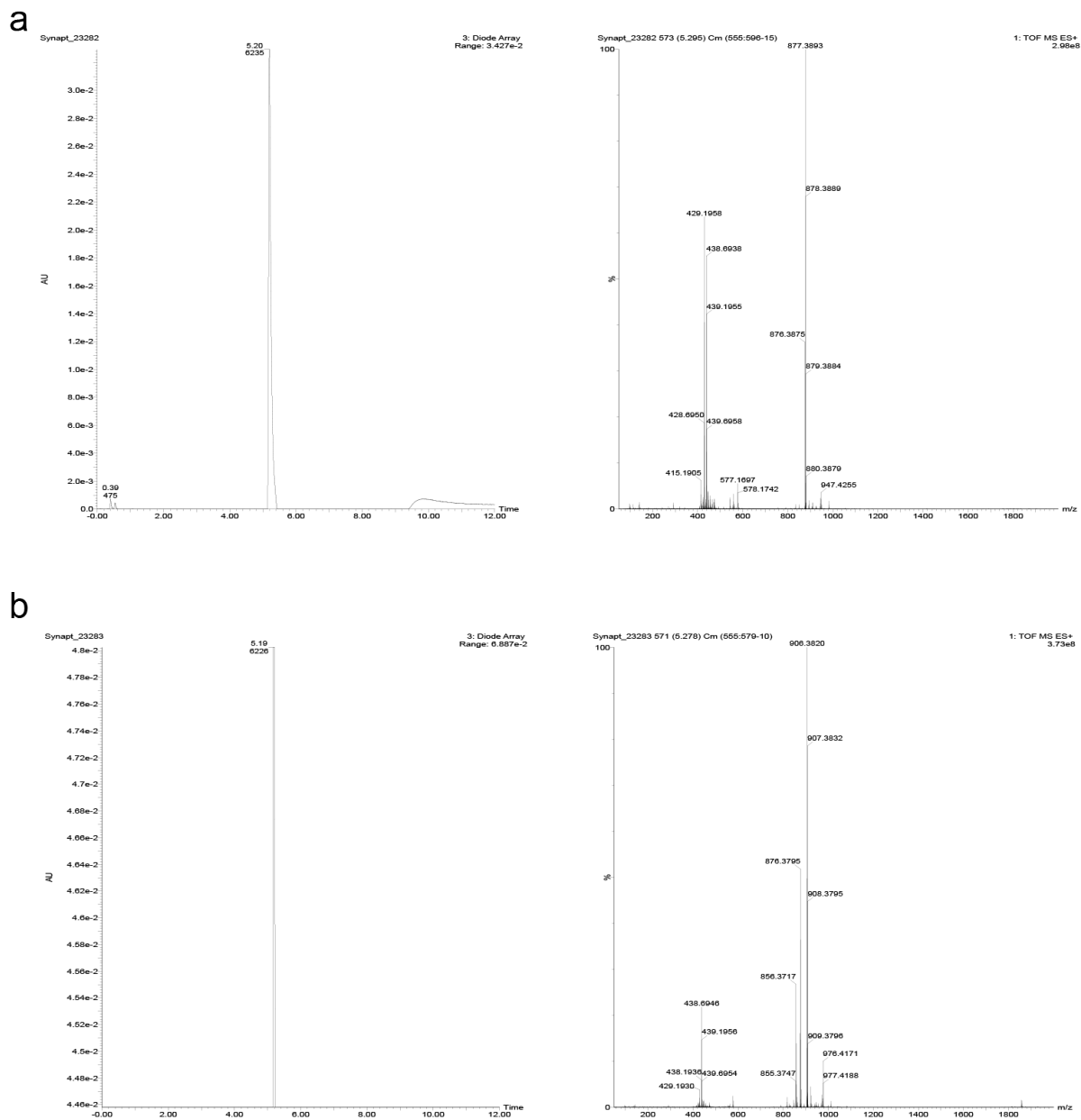


**Figure S4.** LC-HRMS analysis of the crude reaction (a) before and (b) after SR-APNO-1 (167  $\mu\text{M}$ ), and methanolic NO ( $\sim 10$  mM,  $\sim 60$  equiv.) in anhydrous methanol. The reaction was initiated with the addition of saturated methanolic nitric oxide and then allowed to react at room temperature for less than 5 minutes. The solution was purged under high vacuum and then concentrated under vacuum before analysis. Products were separated on a CORTECS<sup>TM</sup> UPLC C18 column (1.6  $\mu\text{m}$ , 2.1 by 50 mm) with a linear gradient using a combination of solvent A (95% water, 5% acetonitrile, 0.1% TFA) and solvent B (95% acetonitrile, 5% water, 0.1% TFA) at a flow rate of 0.4 mL/minute. Linear gradient protocol in minutes: 0 - 1 (80% A); 1 - 4 (40% A); 4 - 8 (100% B); 8 - 8.1 (80% A); and 8.1 - 12 (80% A). LC was monitored using a PDA detector between 350 and 500 nm (left). Identified SR-APNO-1 (calc'd  $[\text{M}]^+$  877.3837, found 877.3893 Da), and t-SR-APNO-1 (calc'd  $[\text{M}]^+$  906.3744, found 906.3820 Da). *N*-nitrosated product was corroborated using ESI-HRMS t-SR-APNO-1 (calc'd  $[\text{M}]^+$  906.3744, found 906.3757 Da).

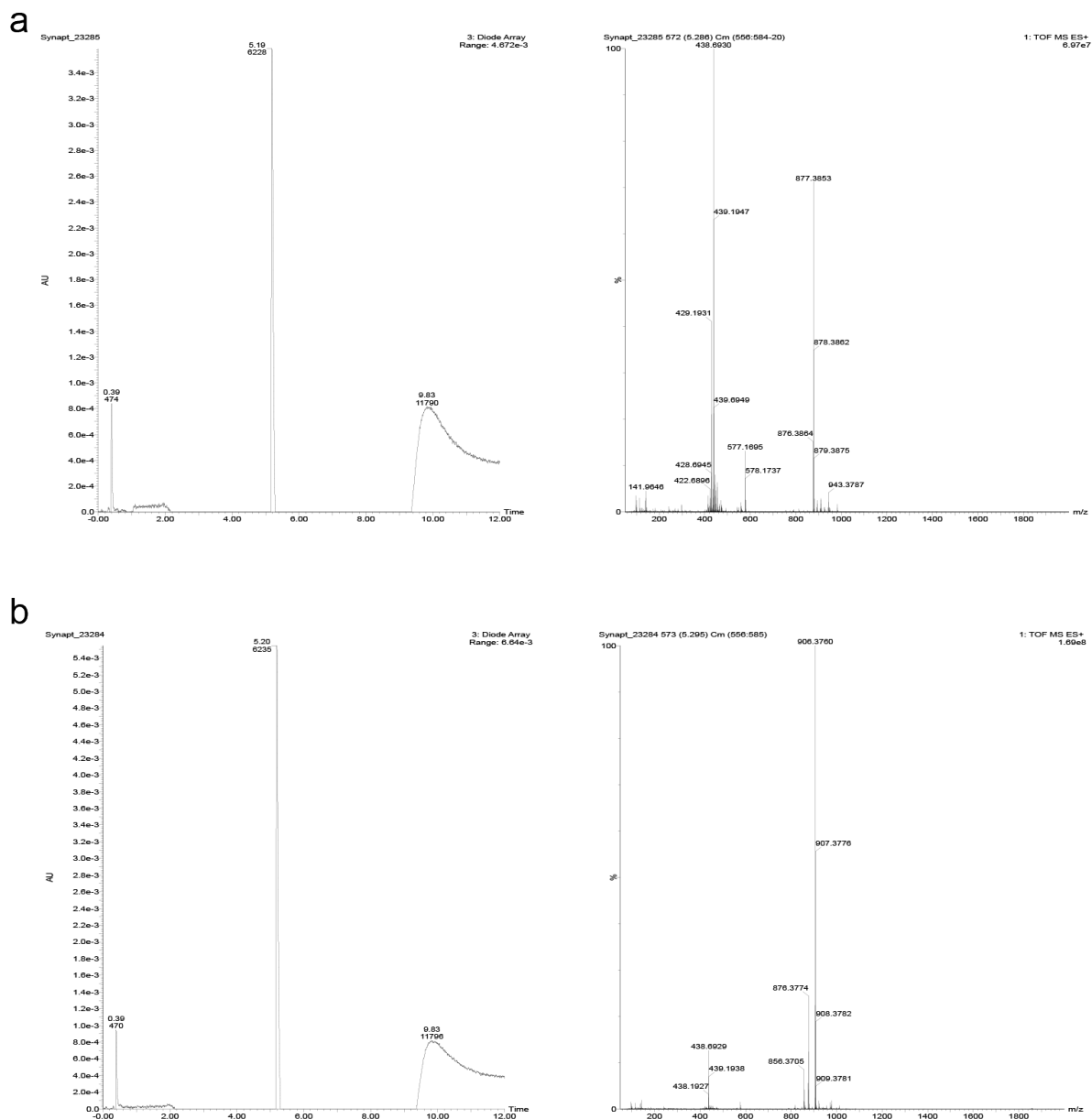


**Figure S5.** LC-HRMS analysis of the crude reaction (a) before and (b) after SR-APNO-2 (167  $\mu$ M), and methanolic NO ( $\sim$ 10 mM,  $\sim$ 60 equiv.) in anhydrous methanol. The reaction was initiated with the addition of saturated methanolic nitric oxide and then allowed to react at room temperature for less than 5 minutes. The solution was purged under high vacuum and then concentrated under vacuum before analysis. Products were separated on a CORTECS<sup>TM</sup> UPLC C18 column (1.6  $\mu$ m, 2.1 by 50 mm) with a linear gradient using a combination of solvent A (95% water, 5% acetonitrile, 0.1% TFA) and solvent B (95% acetonitrile, 5% water, 0.1% TFA) at a flow rate of 0.4 mL/minute. Linear gradient protocol in minutes: 0 - 1 (80% A); 1 - 4 (40% A); 4 - 8 (100% B); 8 - 8.1 (80% A); and 8.1 - 12 (80% A). LC was monitored using a PDA detector between 350 and 500 nm (left). Identified SR-APNO-2 (calc'd  $[M]^+$  877.3845, found 877.3853), t-SR-APNO-2 calc'd  $[M]^+$  906.3744, found 906.3760 Da). *N*-nitrosated product was corroborated using ESI-HRMS t-SR-APNO-2 (calc'd  $[M]^+$  906.3744, found 906.3762 Da).

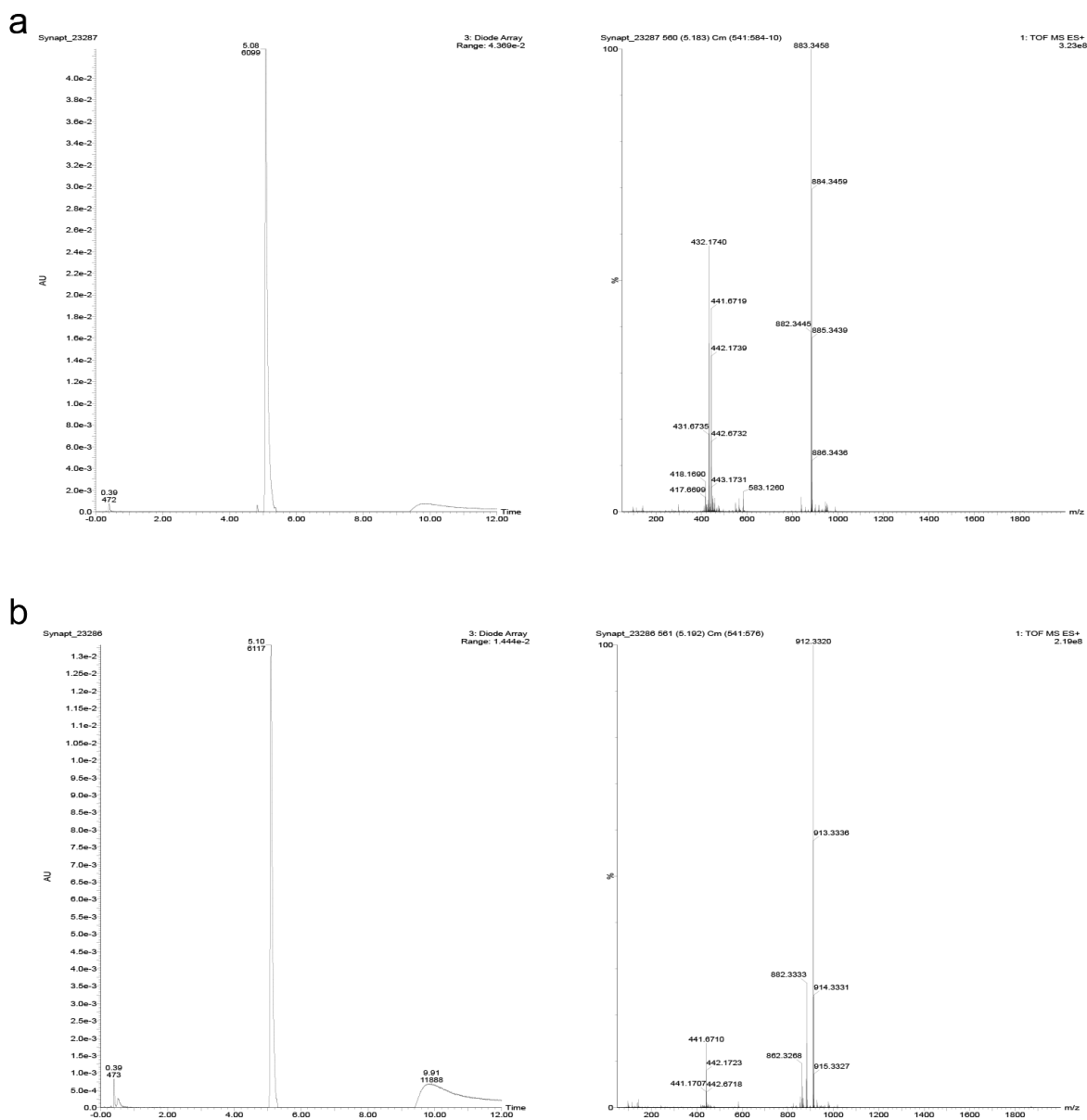


**Figure S6.** LC-HRMS analysis of the crude reaction (a) before and (b) after SR-APNO-3 (167  $\mu$ M), and methanolic NO (~10 mM, ~60 equiv.) in anhydrous methanol. The reaction was initiated with the addition of saturated methanolic nitric oxide and then allowed to react at room temperature for less than 5 minutes. The solution was purged under high vacuum and then concentrated under vacuum before analysis. Products were separated on a CORTECS™ UPLC C18 column (1.6  $\mu$ m, 2.1 by 50 mm) with a linear gradient using a combination of solvent A (95% water, 5% acetonitrile, 0.1% TFA) and solvent B (95% acetonitrile, 5% water, 0.1% TFA) at a flow rate of 0.4 mL/minute. Linear gradient protocol in minutes: 0 - 1 (80% A); 1 - 4 (40% A); 4 - 8 (100% B); 8 - 8.1 (80% A); and 8.1 - 12 (80% A). LC was monitored using a PDA detector between 350 and 500 nm (left). Identified SR-APNO-3 (calc'd  $[M]^+$  883.3047, found 883.3458 Da), t-SR-APNO-3 (calc'd  $[M]^+$  912.3308, found 912.3320 Da). *N*-nitrosated product was corroborated using ESI-HRMS t-SR-APNO-3 (calc'd  $[M]^+$  912.3308, 912.3321 found Da).

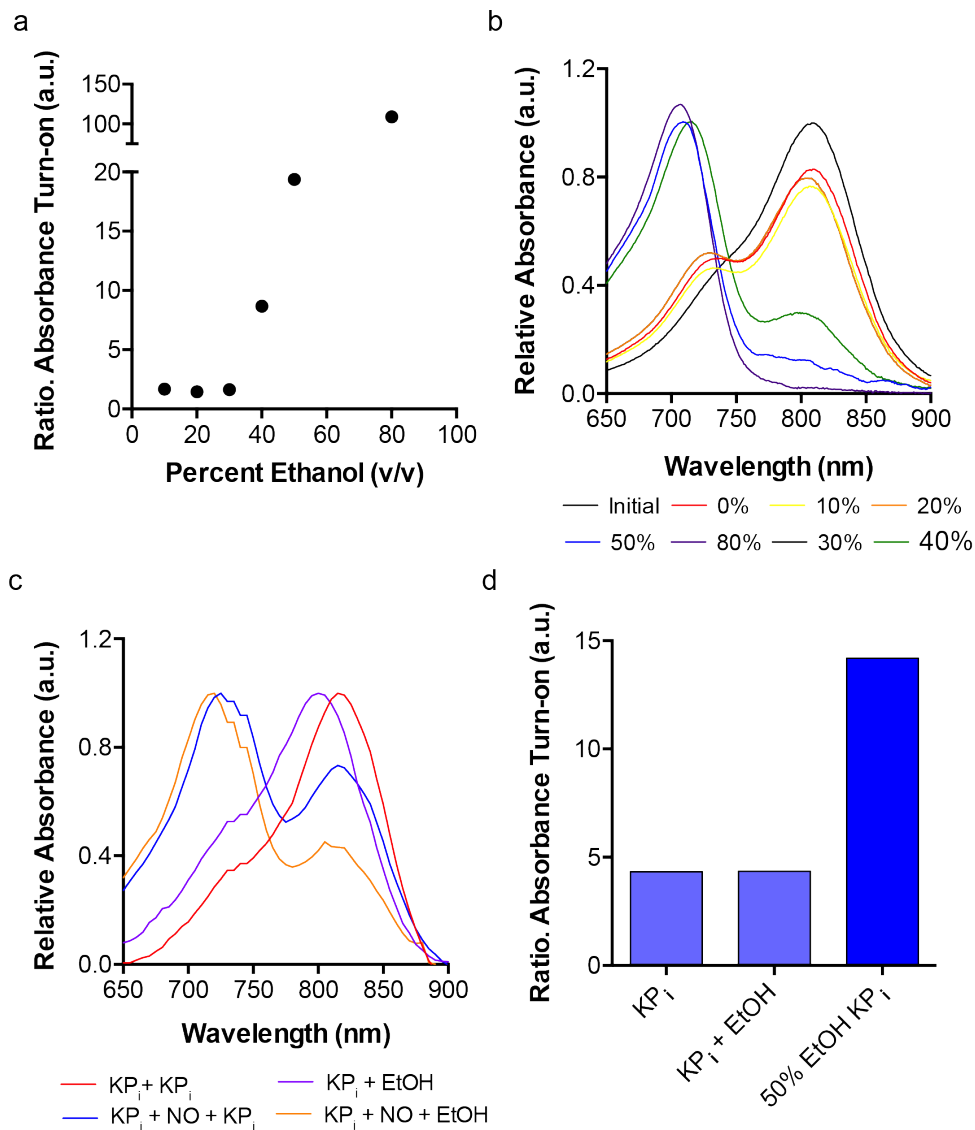


**Figure S7.** Effect of ethanol content in 20 mM potassium phosphate buffer (pH 7.4, 0.1% CrEL v/v) on the (a) ratiometric absorbance response and (b) UV-vis spectra. Reactions were performed with SR-APNO-3 (4  $\mu$ M) and DEA-NONOate (1.33 mM, 2 mM NO) at room temperature for 20 min (approximately 1.25 half-lives). (c) UV-vis spectra and (d) ratiometric absorbance responses for dilution experiments to investigate the source of ethanol effects. Reactions were performed with SR-APNO-3 (4  $\mu$ M) and DEA-NONOate (1.33 mM in 10 mM KOH, 2 mM NO) or control (equal volume 10 mM KOH) in 20 mM potassium phosphate buffer (pH 7.4, 0.1% CrEL v/v) at room temperature for 1 h and then diluted in additional buffer (KP<sub>i</sub>) or ethanol (EtOH).

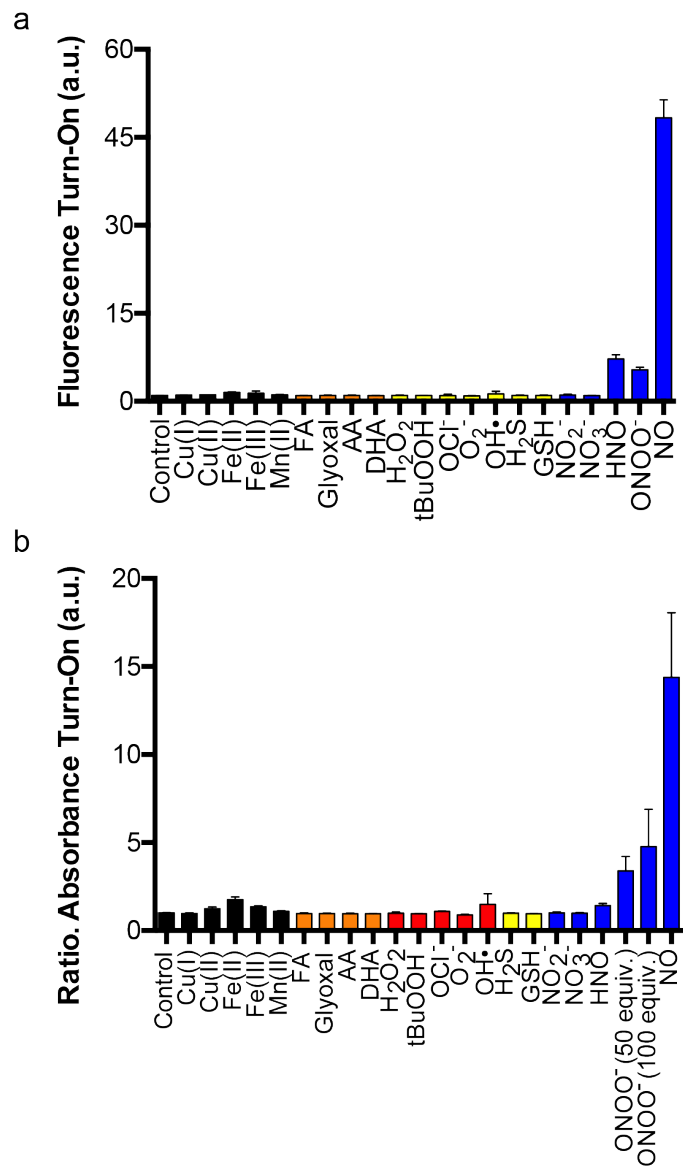


**Figure S8.** (a) Fluorescence and (b) UV-vis analysis of SR-APNO-3's (4  $\mu$ M) selectivity against a panel of reactive metals (black), carbonyl (orange), oxygen (red), thiol (yellow) and nitrogen (blue) species (800  $\mu$ M, 200 equiv. unless noted otherwise) in ethanolic 20 mM potassium phosphate buffer (pH 7.4, 50% v/v) or ethanolic 20 mM HEPES buffer (pH 7.4, 50% v/v, Fe(II) only). Minor fluorescence enhancement (less than 15% of NO response) was observed after treatment with HNO. This, along with the lack of change in UV-vis, is consistent with the small quantities of NO that are released from Angeli's salt (the nitroxyl donor).<sup>18</sup> Note that the slight response from peroxynitrite is only observed in the UV-vis due to dye decomposition after treatment with minor reactivity from residual isoamyl nitrite. Data is reported as the mean  $\pm$  standard deviation ( $n = 3$ ).

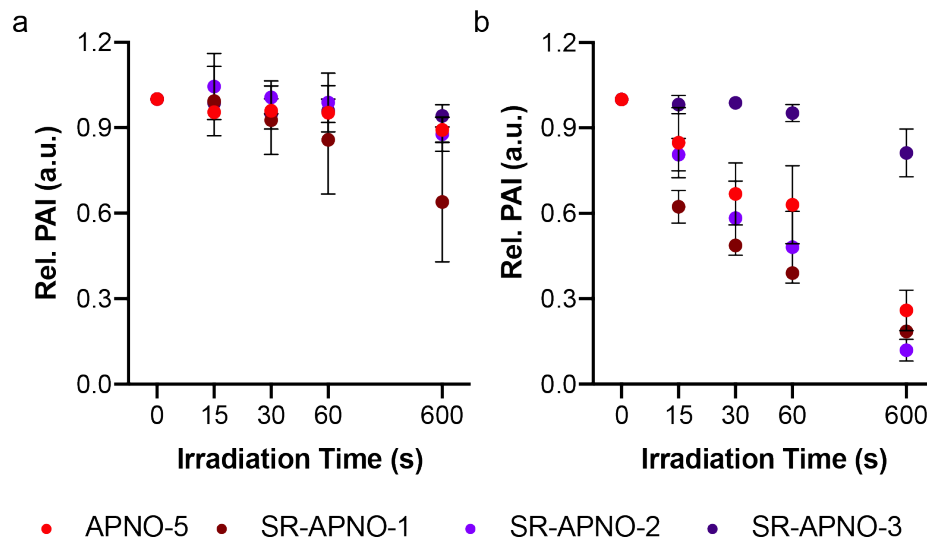


**Figure S9.** APNO or SR-APNO and corresponding *N*-nitrosated product (25  $\mu$ M) photostability at their PA maximum in ethanolic 20 mM potassium phosphate buffer (pH 7.4, 50% v/v) using the OPO laser used in the Nexus 128+ PA tomographer. Samples were irradiated discontinuously, and measurements were acquired in continuous mode with a 6 s rotation time. Data is reported as the mean  $\pm$  standard deviation ( $n = 3$ ).

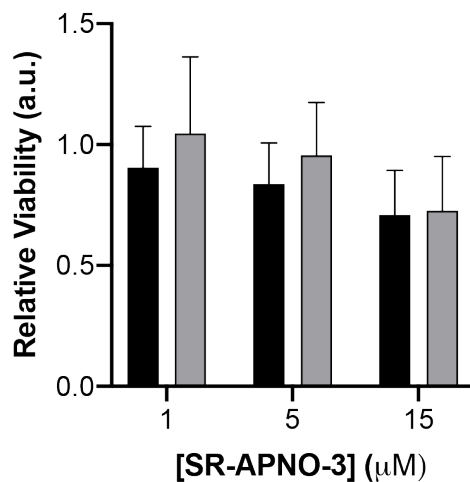


**Figure S10.** MTT toxicity assay for SR-APNO-3 in 4T1 mouse mammary carcinoma cells (black, 24 h) and RAW 264.7 macrophages (grey, 8 h). Data is reported as the mean  $\pm$  standard deviation ( $n = 4$ ).

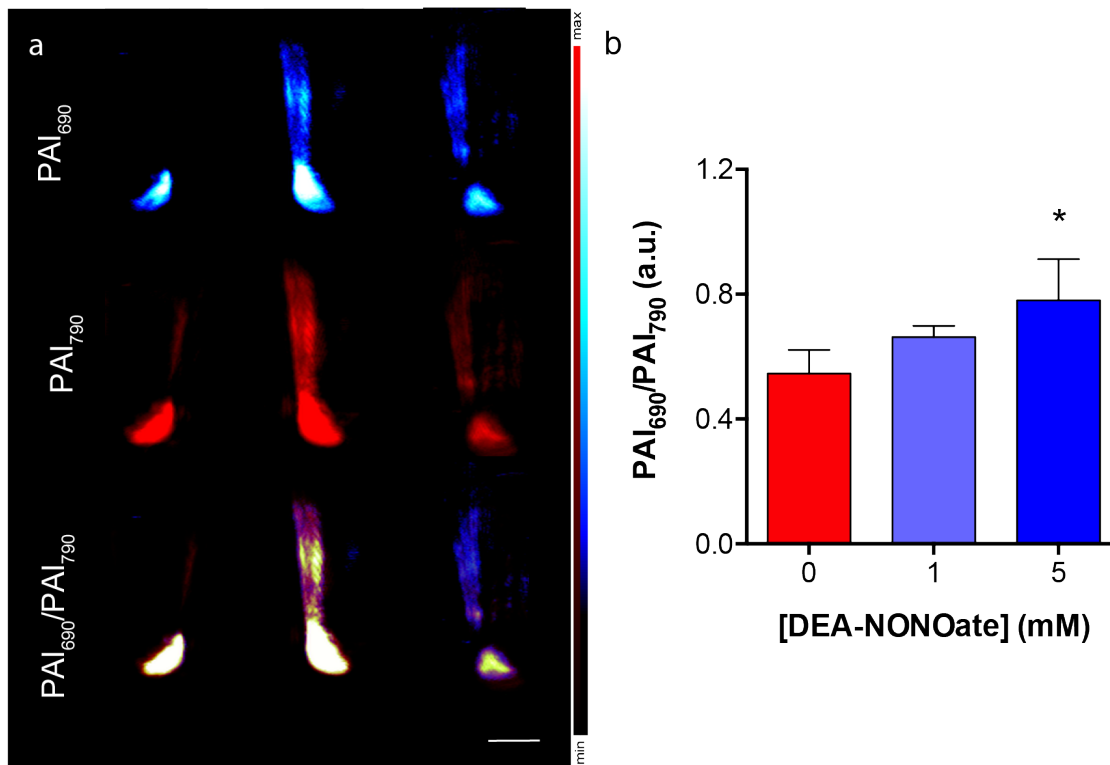


**Figure S11.** (a) PA imaging of 4T1 murine breast cancer cells stained with SR-APNO-3 (15  $\mu$ M) for 1 h, washed with PBS, and then treated with DEA-NONOate for 2 h (1 or 5 mM). Representative images corresponding to the *N*-nitroso product (blue, 690 nm, top), SR-APNO-3 (red, 790 nm, middle), and the image fusion (blue/red, 690/790 nm, bottom). (b) Quantified ratiometric PA response for the cell pellets. Statistical analysis was performed using a one-way ANOVA and Tukey's multiple comparisons ( $\alpha = 0.05$ ). \*,  $p < 0.05$ . Data is reported as the mean  $\pm$  standard deviation ( $n = 3$ ). Scale bar represents 4.0 mm.

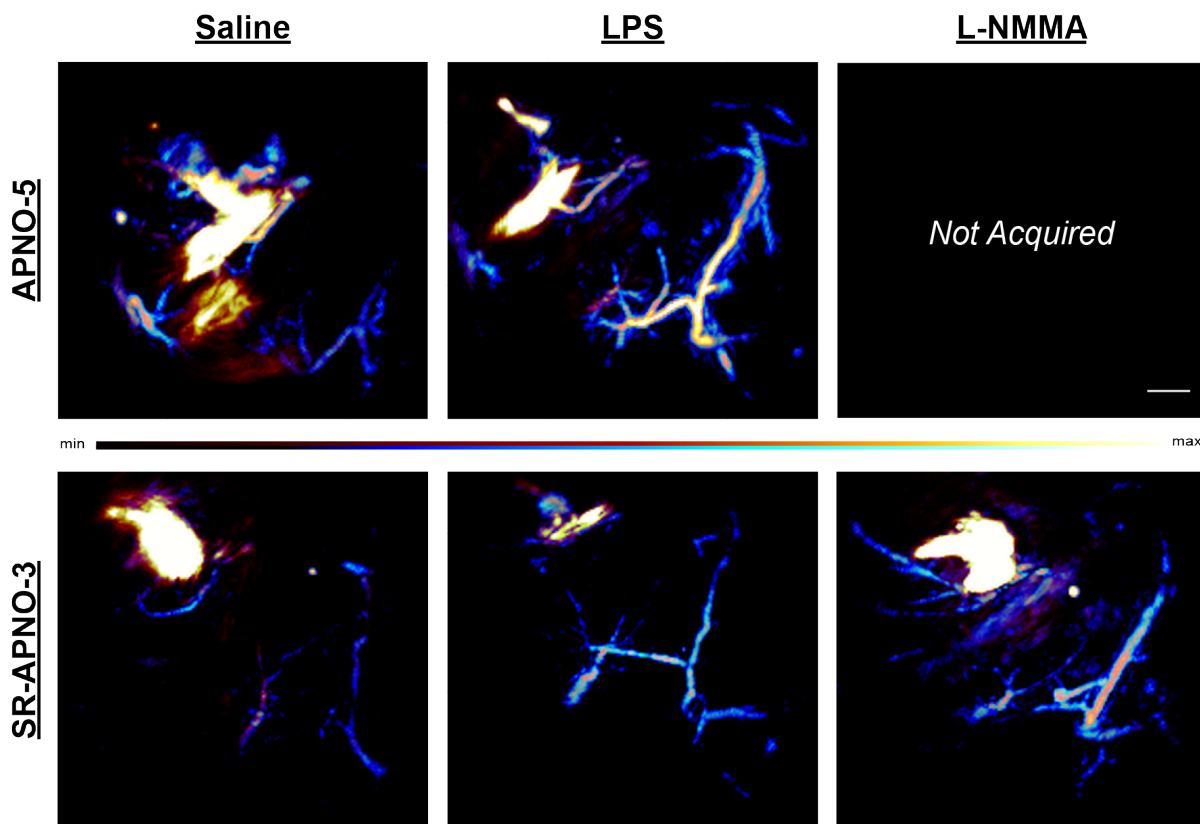


**Figure S12.** PA imaging of LPS-induced inflammation (4 mg/kg, i.m.) in BALB/c mice with APNO-5 (top) and SR-APNO-3 (bottom). After a 4 h induction period, APNO-5 or SR-APNO-3 (50  $\mu$ M, 25  $\mu$ L, i.m., final concentration of 15% DMF v/v) was administered. Inhibition was performed using L-NMMA (35 mM). Representative images correspond to saline- (left), LPS- (middle) and LPS and L-NMMA-treated mice. The *N*-nitroso product (blue, 690 nm) and SR-APNO-3 (red, 790 nm), are shown in a merged image (blue/red, 690/790 nm). Scale bar represents 2.0 mm.

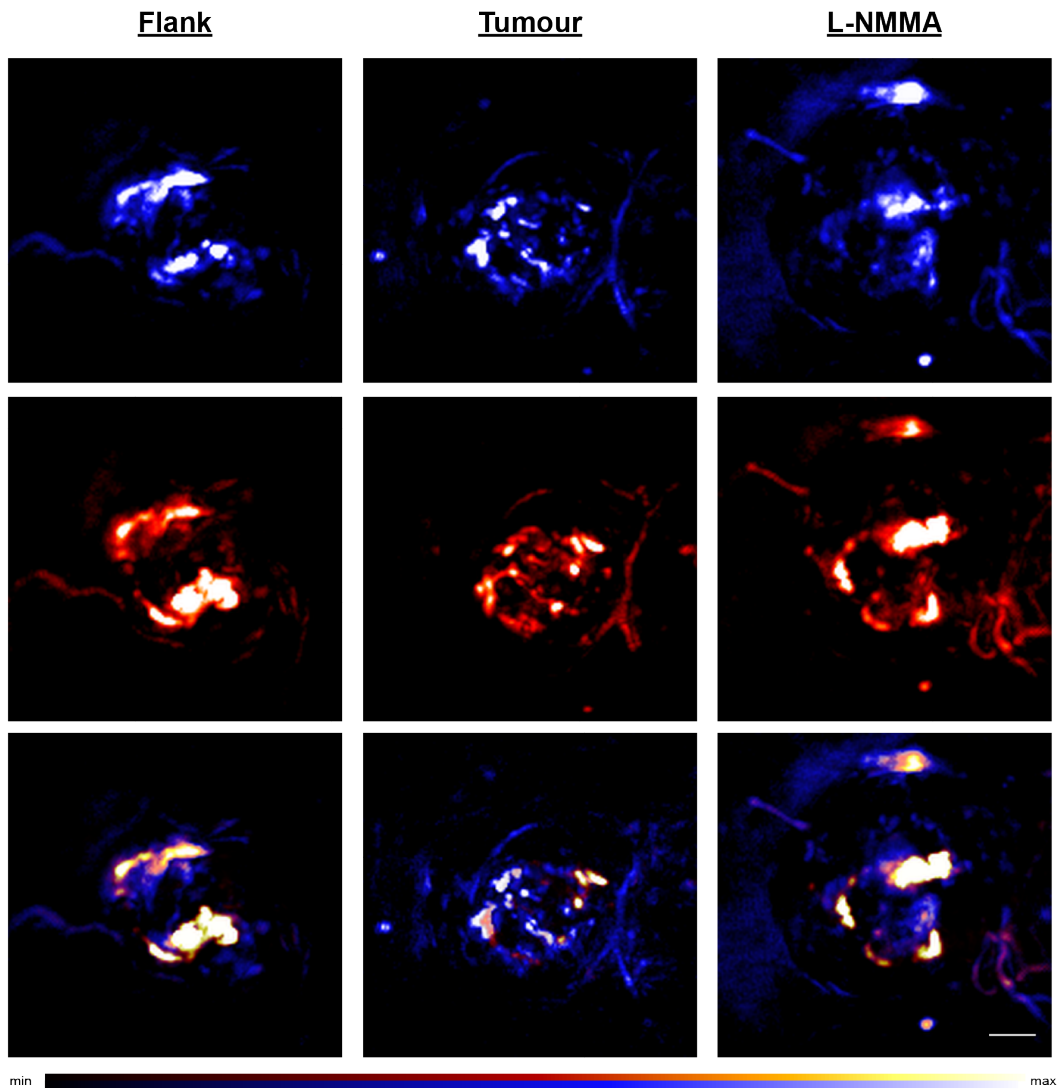


**Figure S13.** PA imaging of cancer-derived NO in a 4T1 heterotopic allograft model of breast cancer. SR-APNO-3 (50  $\mu$ M, 25  $\mu$ L, final concentration of 15% DMF v/v) was administered either subcutaneously or intratumorally. Inhibition was performed using L-NMMA (35 mM). Representative images correspond to the *N*-nitroso product (blue, 690 nm, top), SR-APNO-3 (red, 790 nm, middle), and merged images (blue/red, 690/790 nm, bottom). Scale bar represents 2.0 mm.

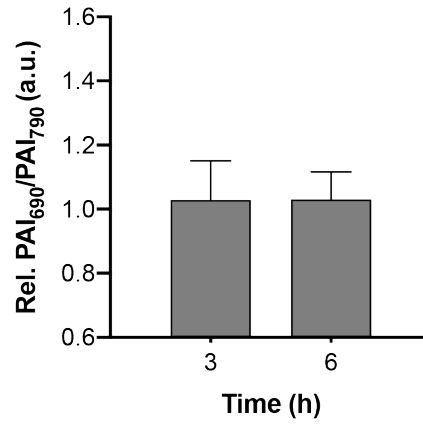


**Figure S14.** PA imaging of 4T1 tumours following intratumoral treatment with 35 mM L-NMMA in sterile saline with 15% DMF. No change in signal was observed in the absence of SR-APNO-3. Data is reported as the mean  $\pm$  standard deviation ( $n = 3$ ).

NMR Spectroscopic Data.

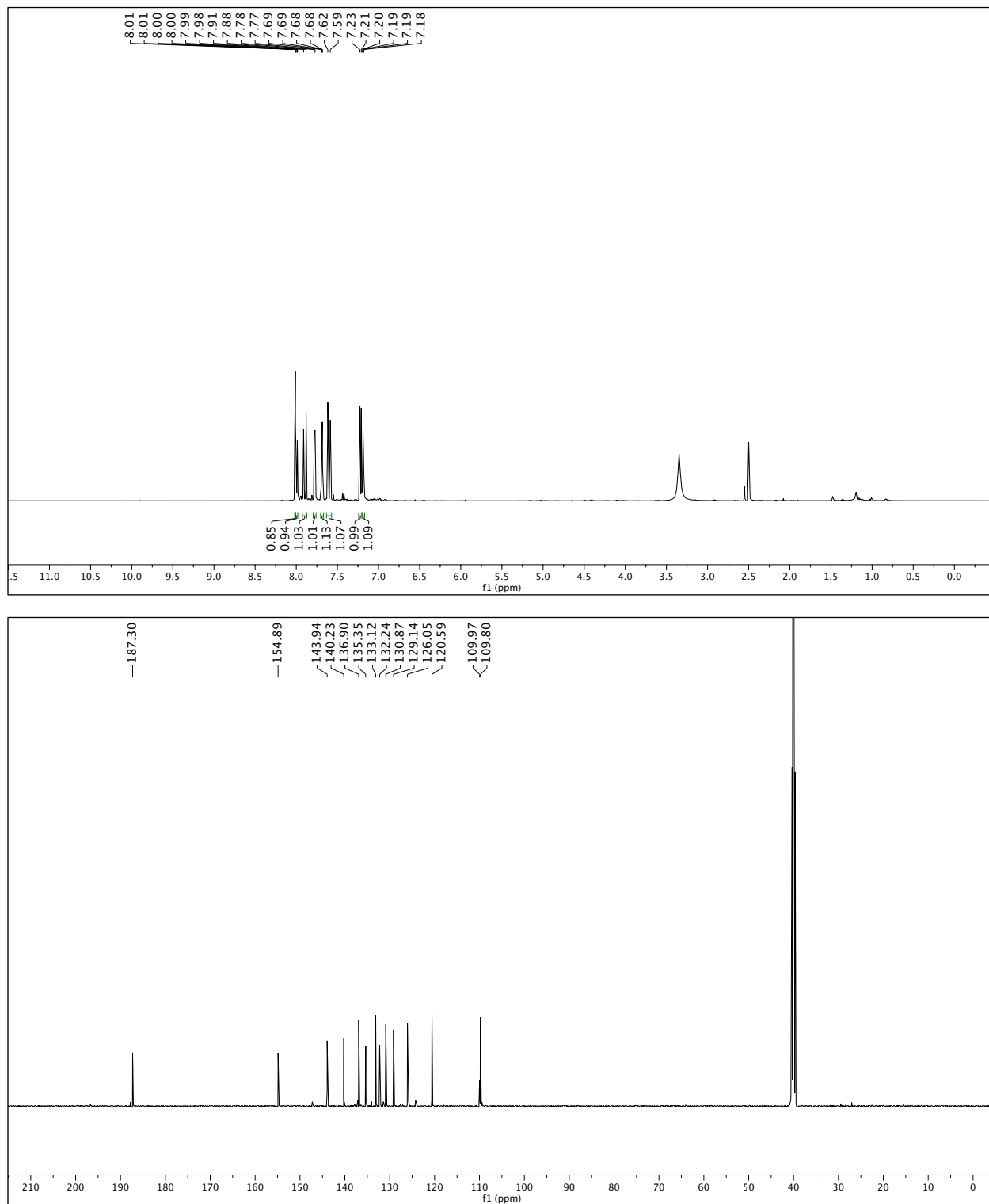
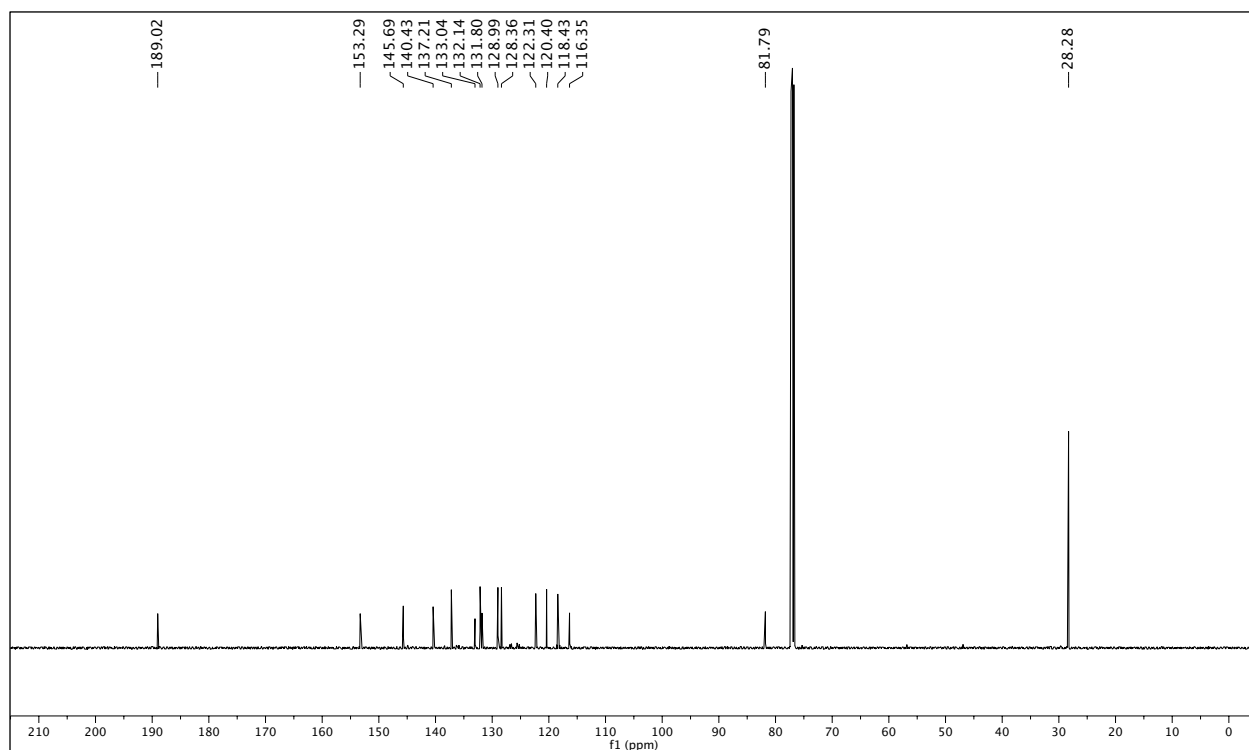
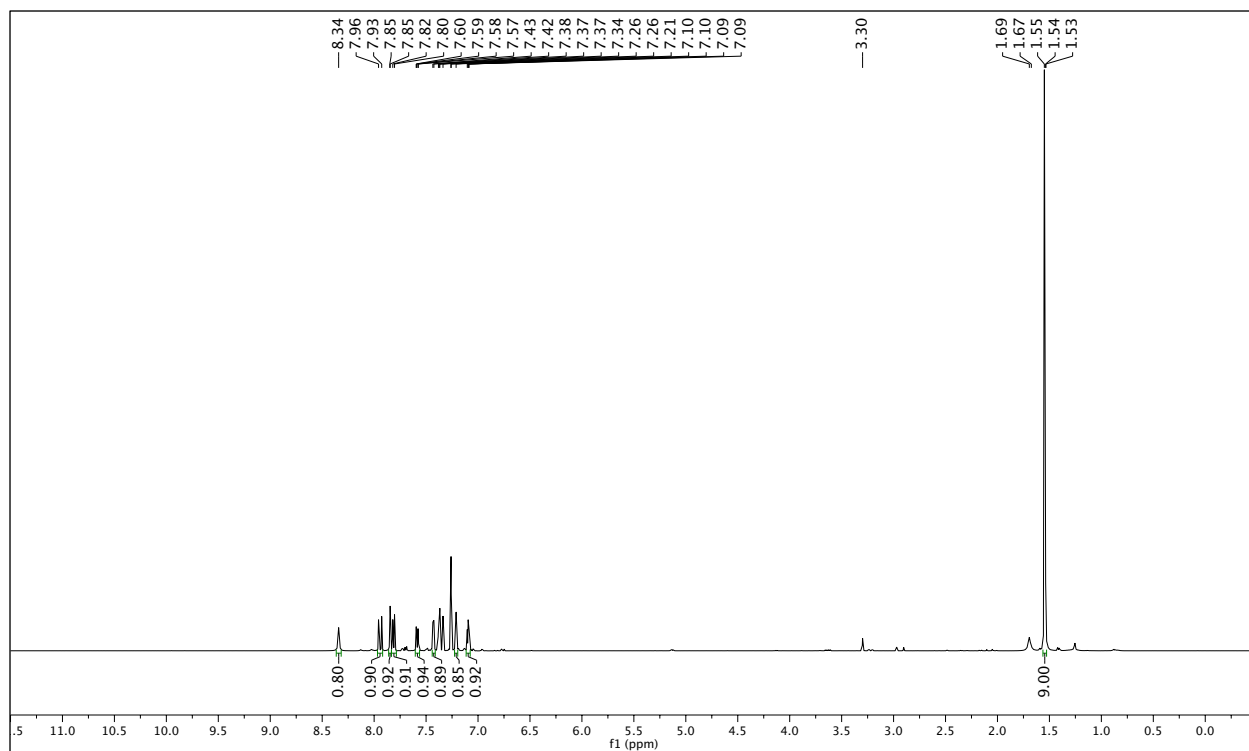


Figure S15.  $^1\text{H}$  NMR (500 MHz,  $\text{DMSO-}d_6$ ) and  $^{13}\text{C}$  NMR (125 MHz,  $\text{DMSO-}d_6$ ) spectra of compound 2.



**Figure S16.** <sup>1</sup>H NMR (500 MHz, CDCl<sub>3</sub>) and <sup>13</sup>C NMR (125 MHz, CDCl<sub>3</sub>) spectra of compound **3**.

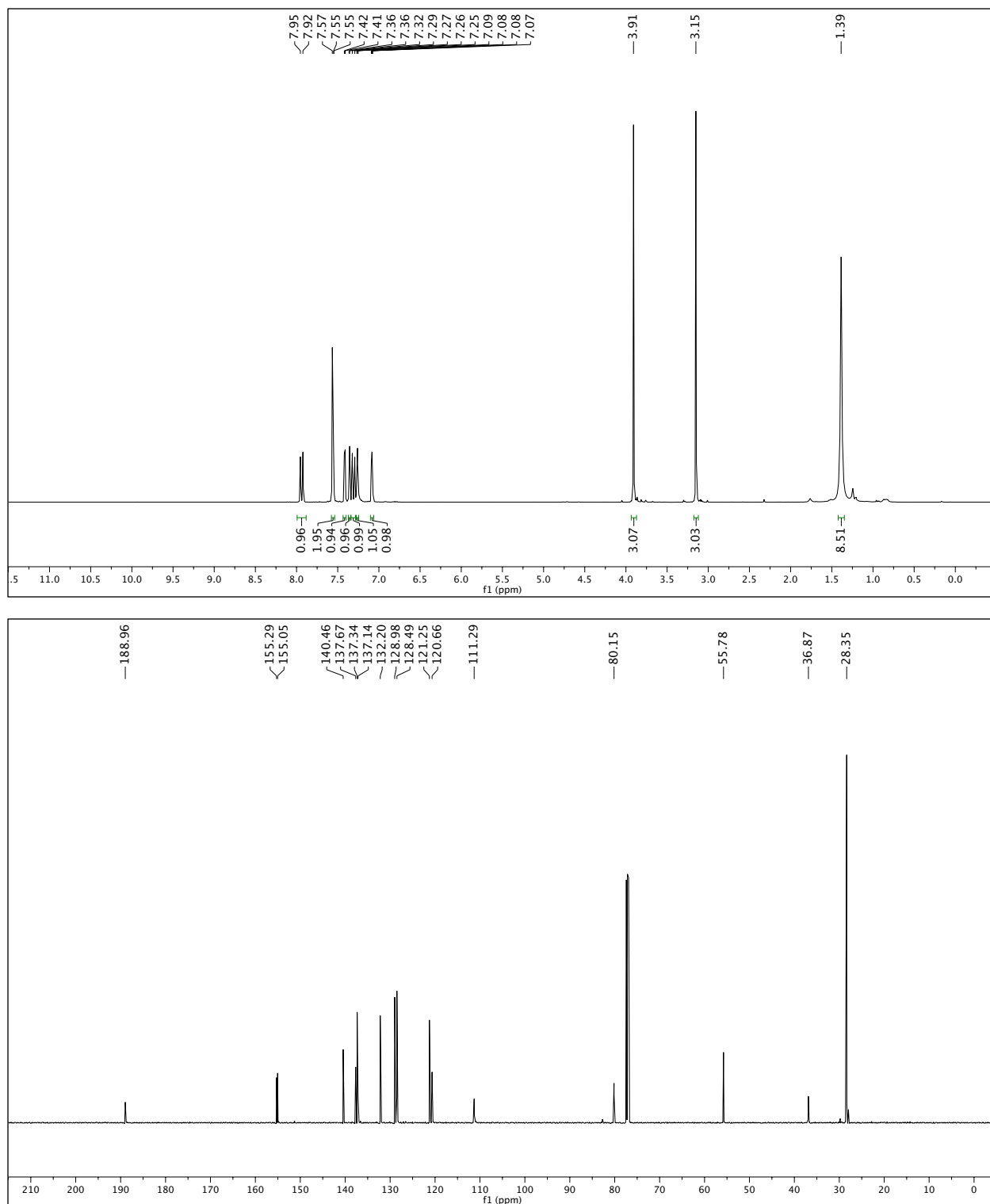
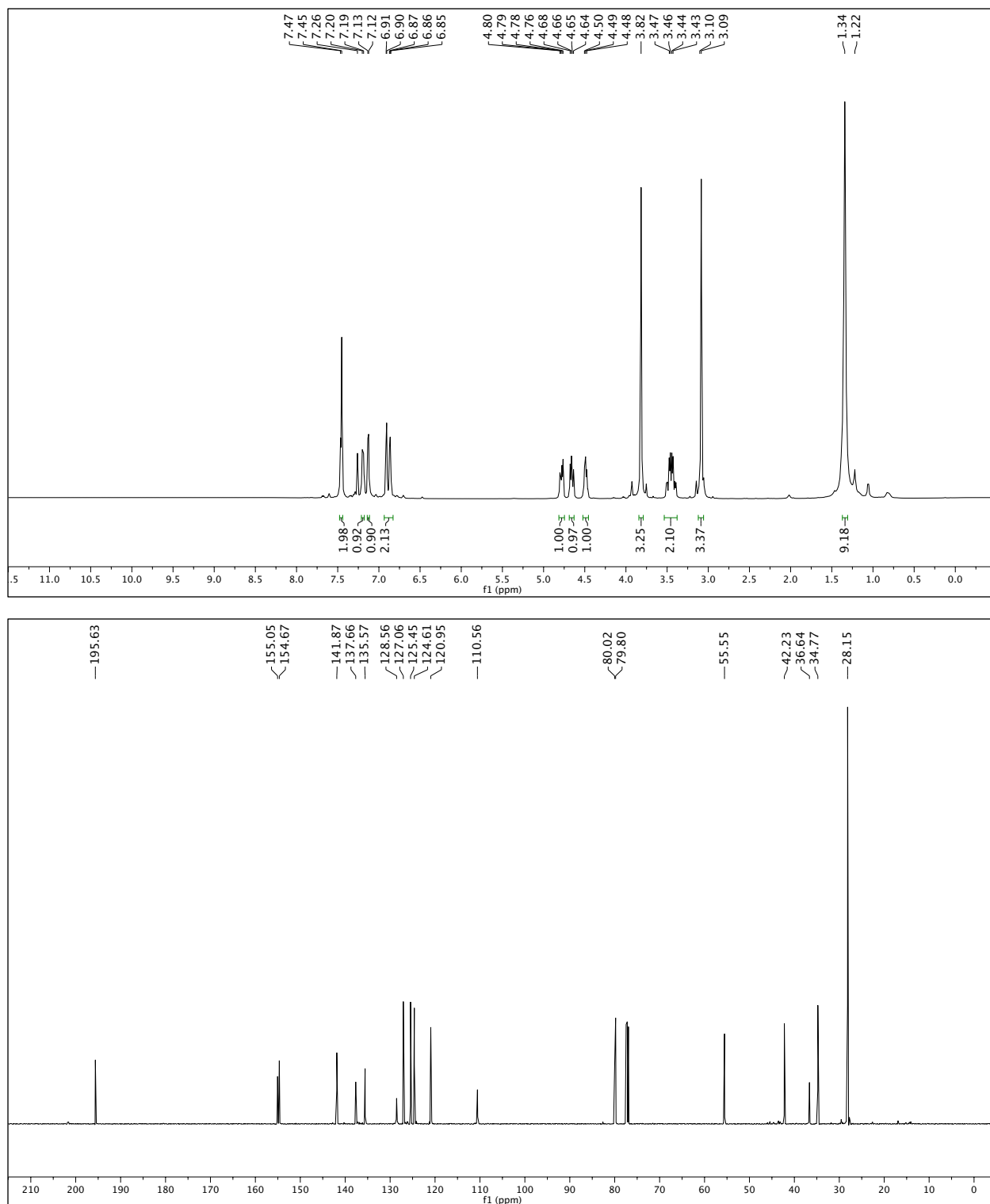
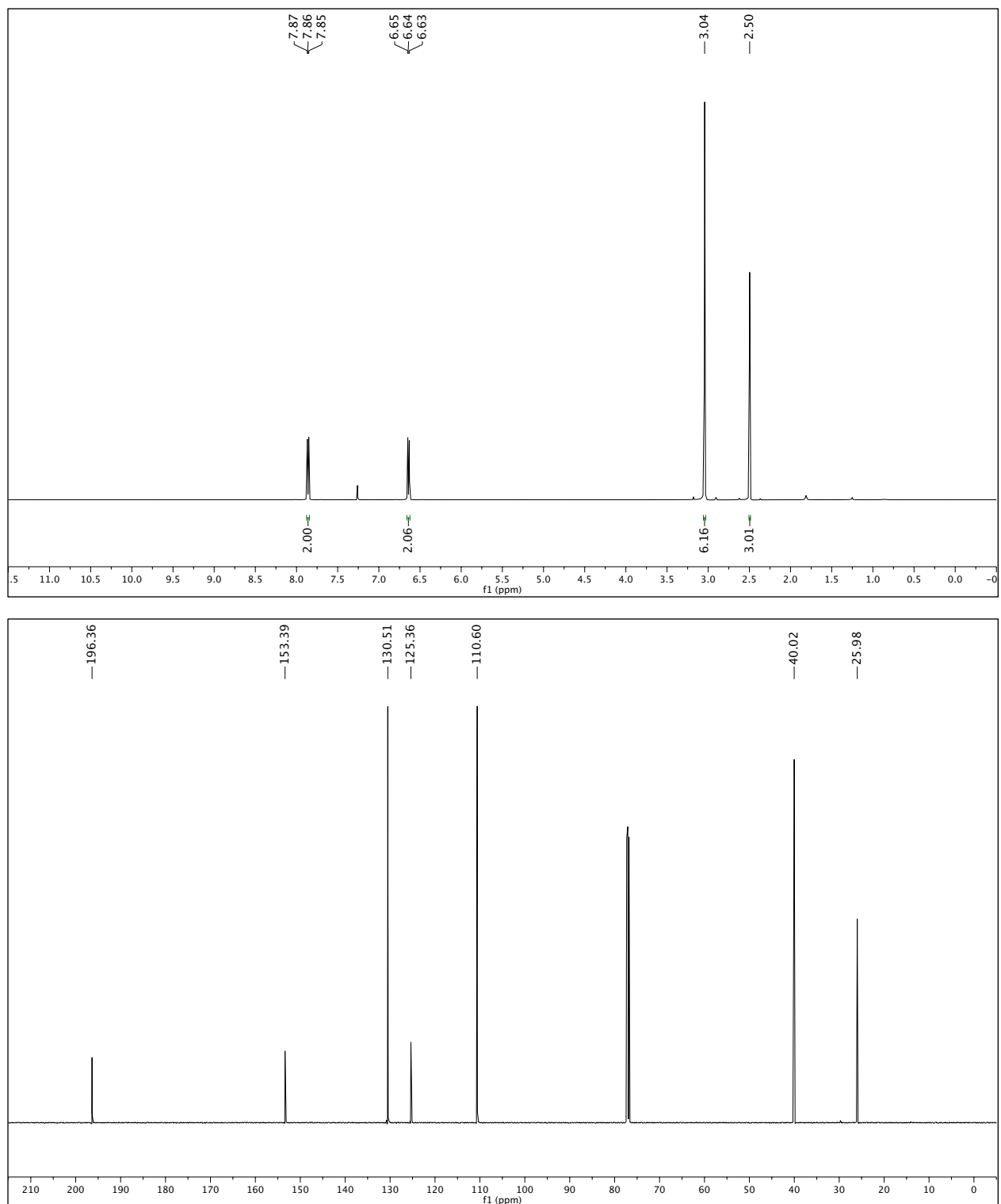


Figure S17. <sup>1</sup>H NMR (500 MHz, CDCl<sub>3</sub>) and <sup>13</sup>C NMR (125 MHz, CDCl<sub>3</sub>) spectra of compound 4.



**Figure S18.** <sup>1</sup>H NMR (500 MHz, CDCl<sub>3</sub>) and <sup>13</sup>C NMR (125 MHz, CDCl<sub>3</sub>) spectra of compound **5**.



**Figure S19.** <sup>1</sup>H NMR (500 MHz, CDCl<sub>3</sub>) and <sup>13</sup>C NMR (125 MHz, CDCl<sub>3</sub>) spectra of compound **6**.

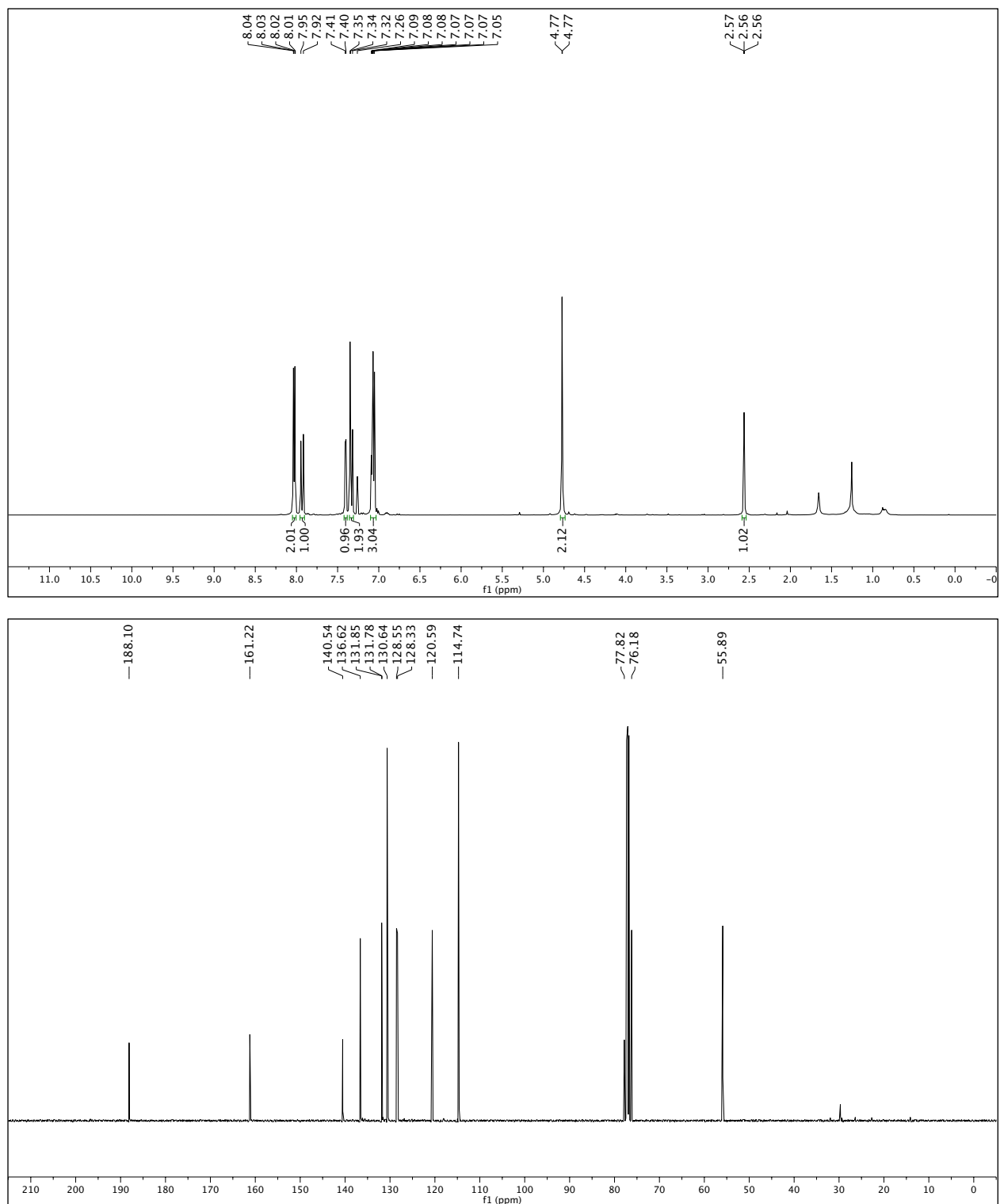


**Figure S20.** <sup>1</sup>H NMR (500 MHz, CDCl<sub>3</sub>) and <sup>13</sup>C NMR (125 MHz, CDCl<sub>3</sub>) spectra of compound **7**.

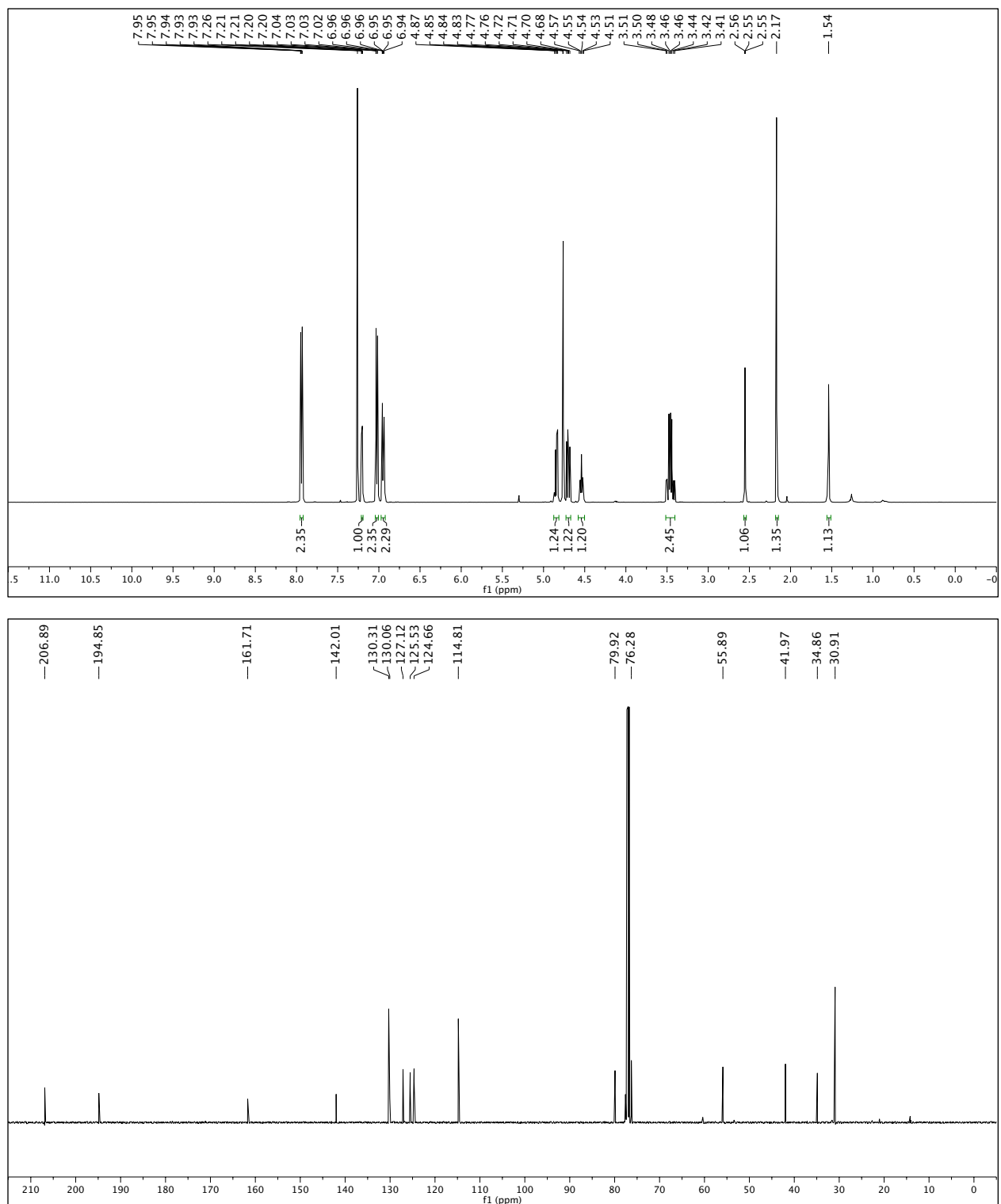


**Figure S21.**  $^1\text{H}$  NMR (500 MHz,  $\text{CDCl}_3$ ) and  $^{13}\text{C}$  NMR (125 MHz,  $\text{CDCl}_3$ ) spectra of compound **8**.

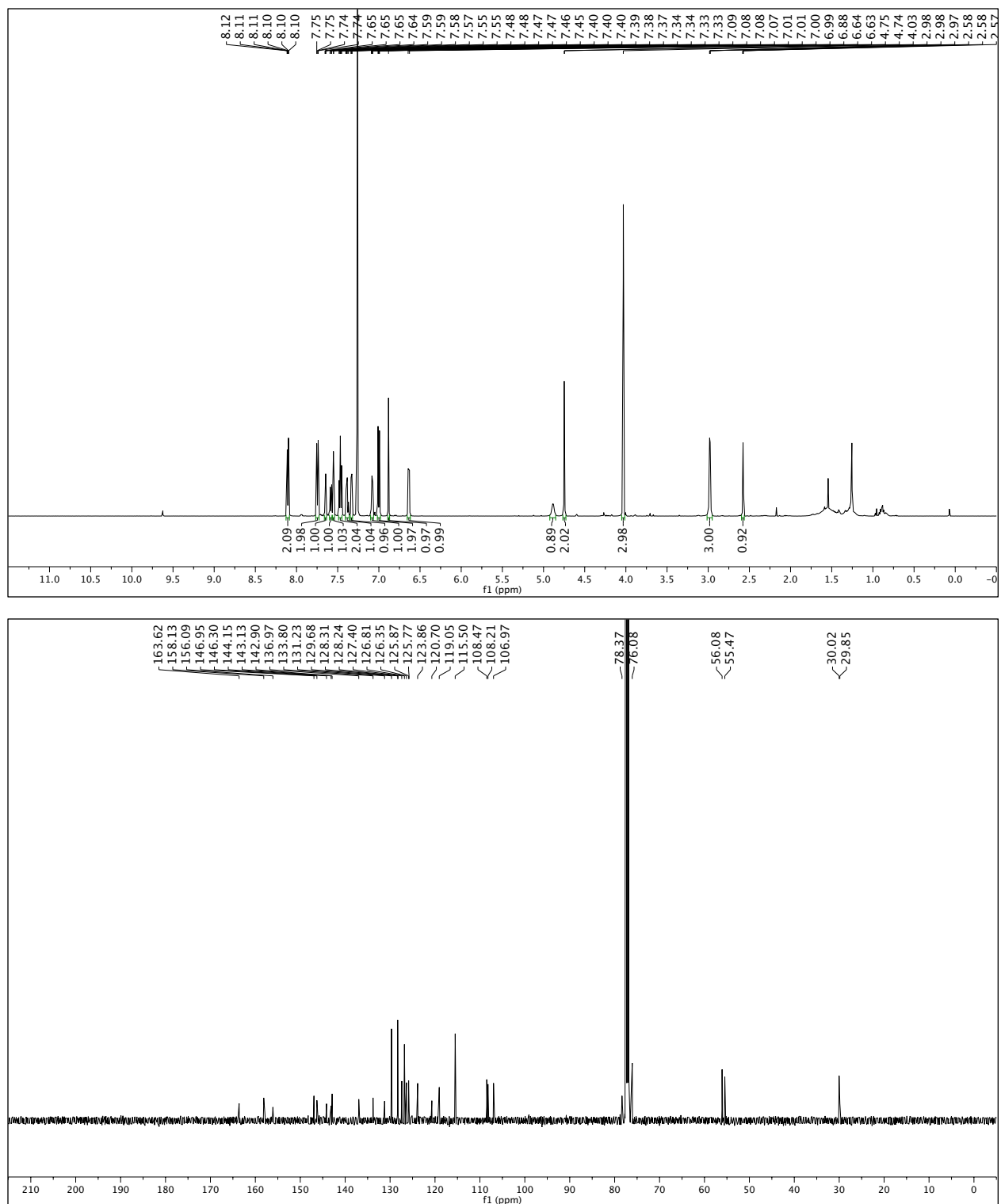


Figure S22.  $^1\text{H}$  NMR (500 MHz,  $\text{CDCl}_3$ ) and  $^{13}\text{C}$  NMR (125 MHz,  $\text{CDCl}_3$ ) spectra of compound 9.

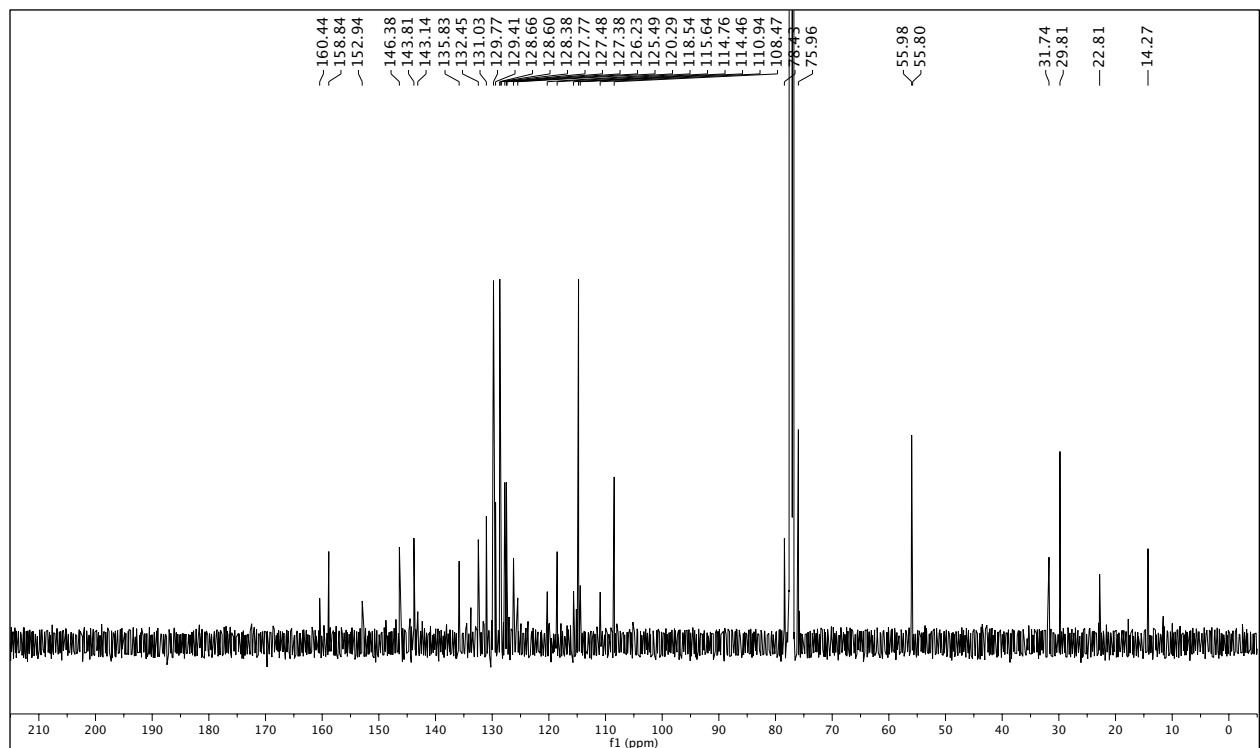
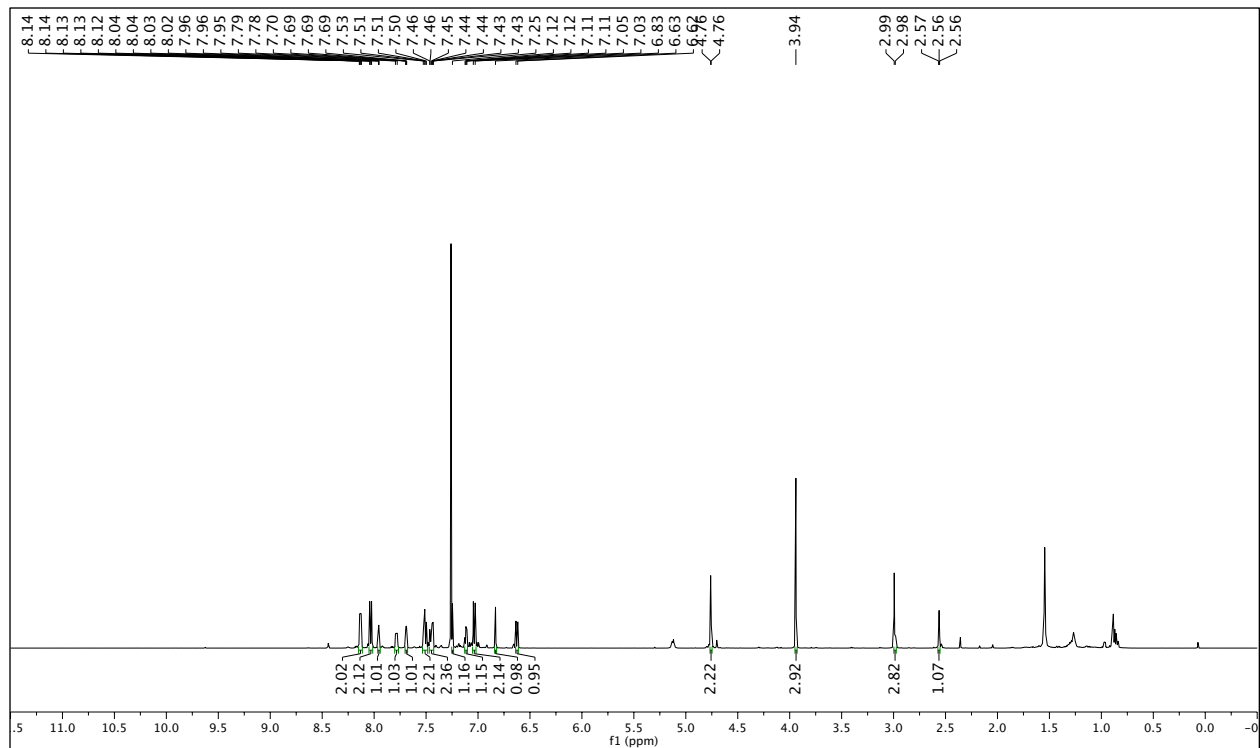
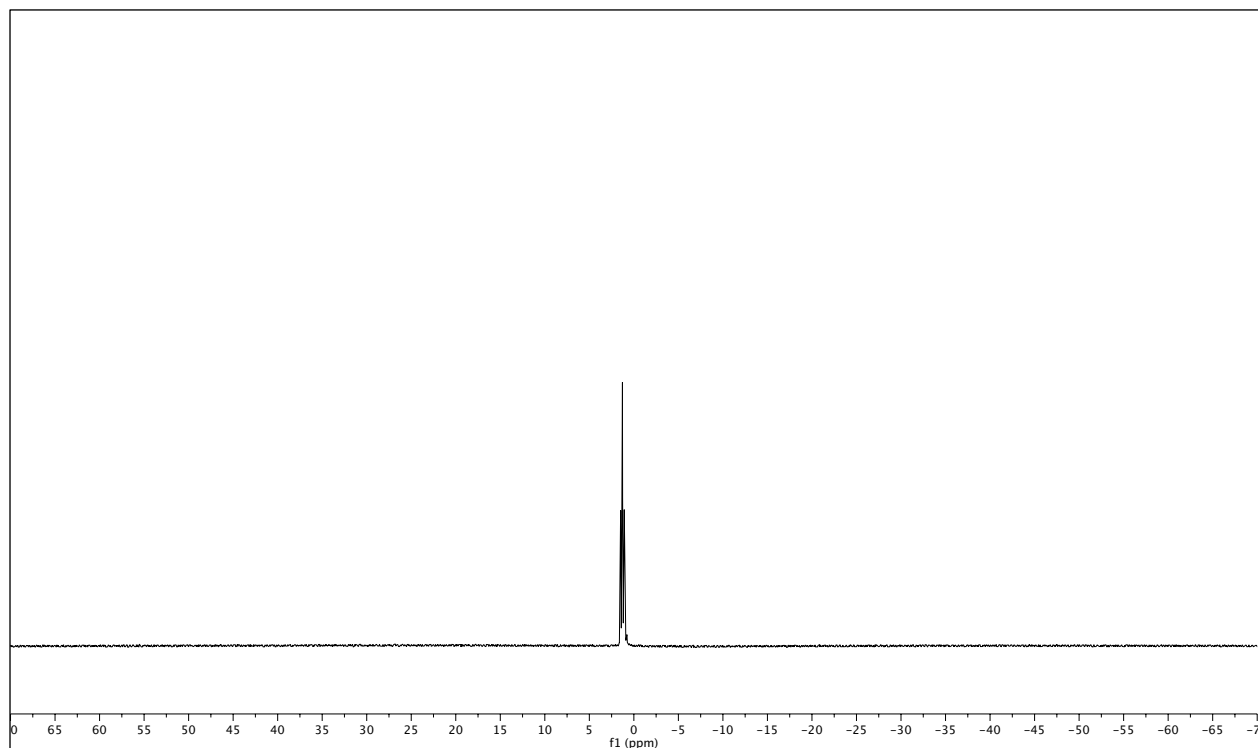
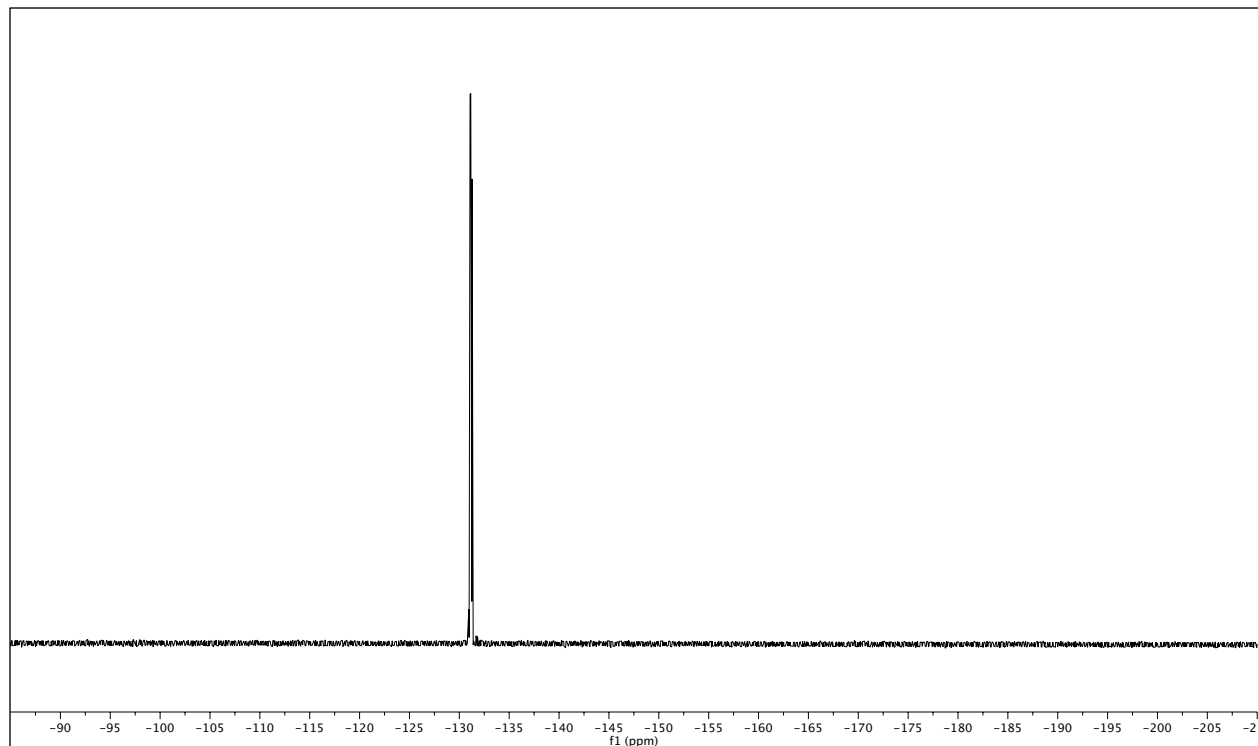
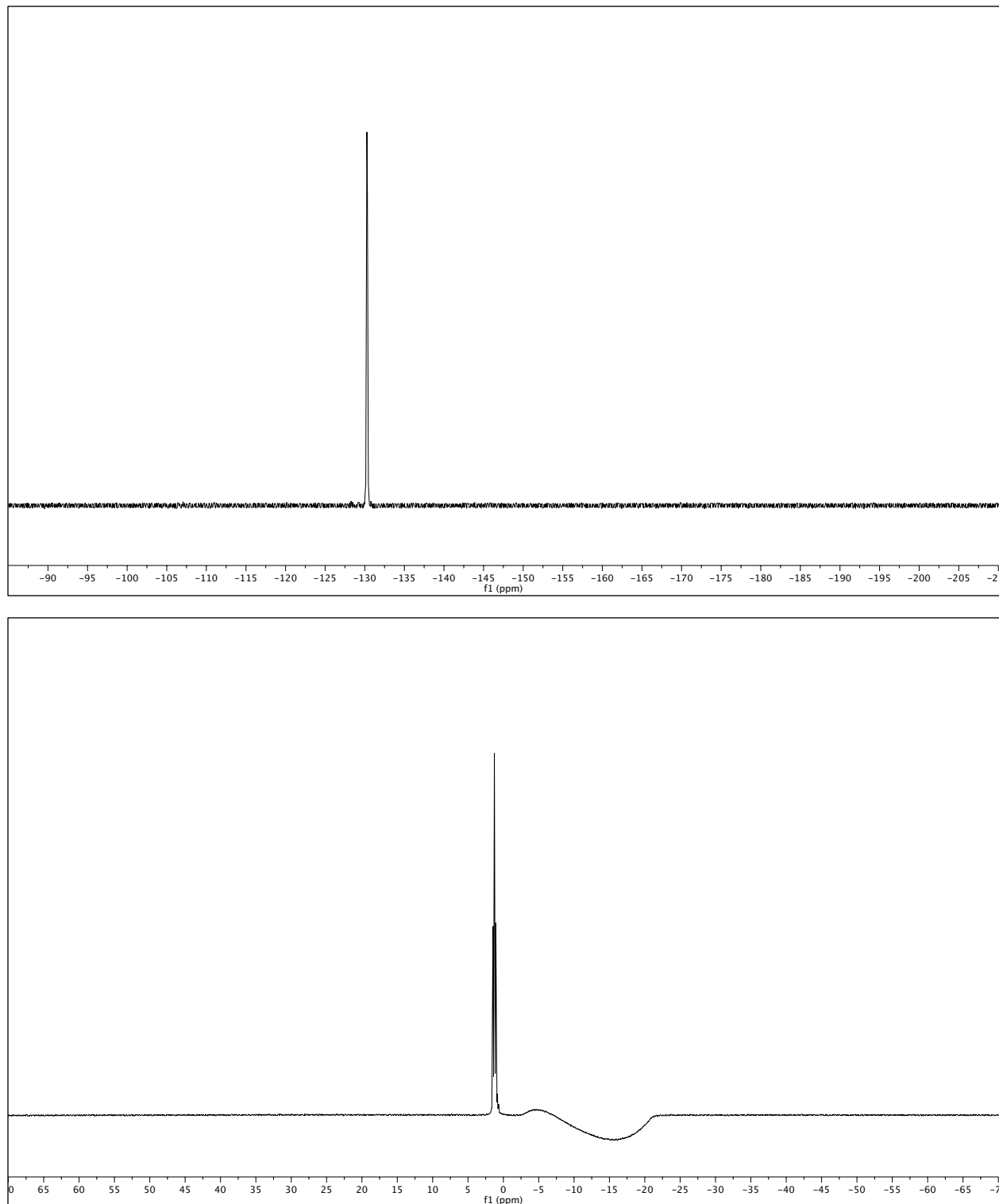


Figure S23.  $^1\text{H}$  NMR (500 MHz,  $\text{CDCl}_3$ ) and  $^{13}\text{C}$  NMR (125 MHz,  $\text{CDCl}_3$ ) spectra of compound **10**.



**Figure S24.**  $^{19}\text{F}$  NMR (471 MHz,  $\text{CDCl}_3$ ) and  $^{11}\text{B}$  NMR (161 MHz,  $\text{CDCl}_3$ ) spectra of compound **10**.





**Figure S26.**  $^{19}\text{F}$  NMR (471 MHz,  $\text{CD}_2\text{Cl}_2$ ) and  $^{11}\text{B}$  NMR (161 MHz,  $\text{CD}_2\text{Cl}_2$ ) spectra of **SR-APNO-1**.

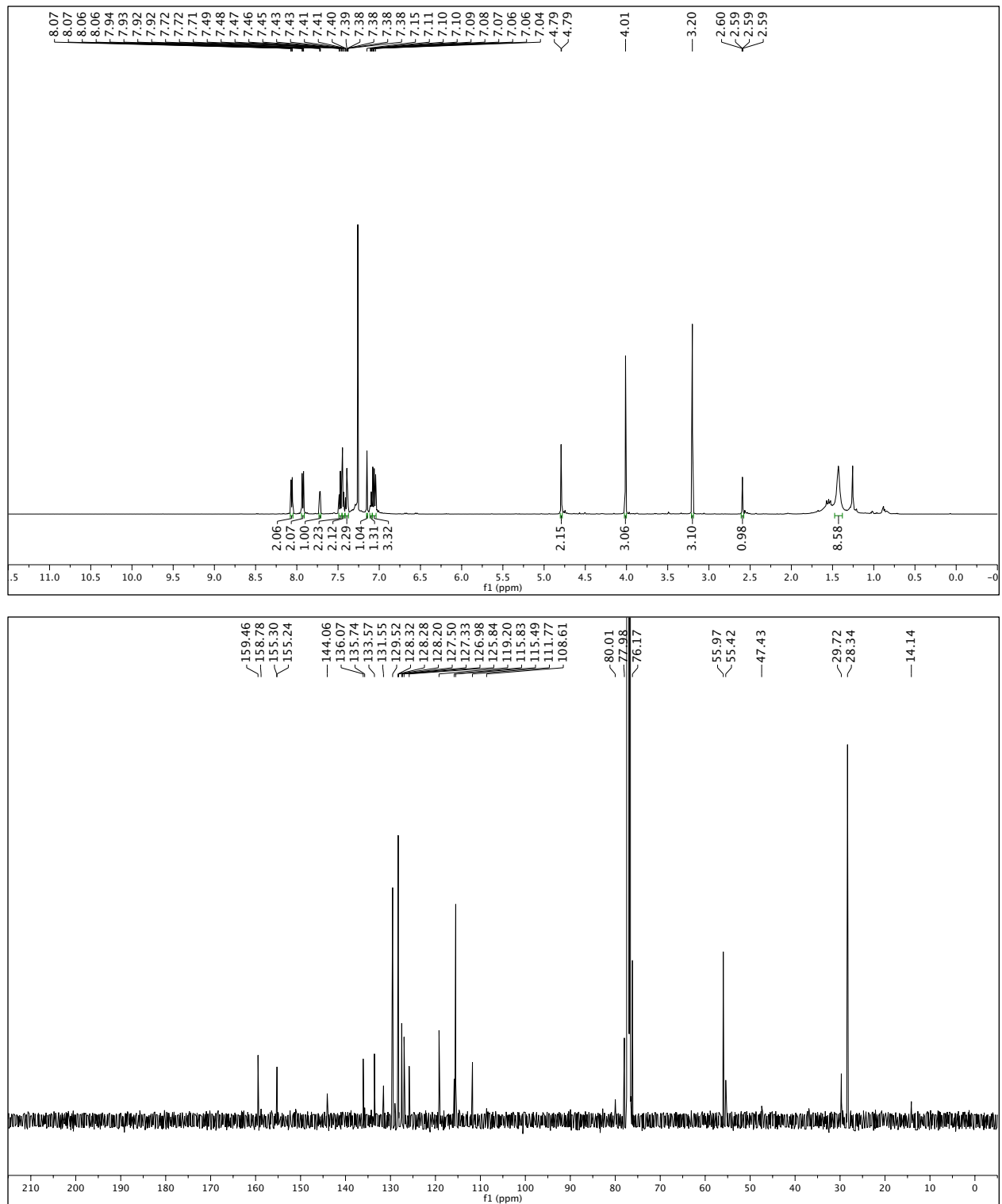


Figure S27. <sup>1</sup>H NMR (500 MHz, CDCl<sub>3</sub>) and <sup>13</sup>C NMR (125 MHz, CDCl<sub>3</sub>) spectra of compound 11.

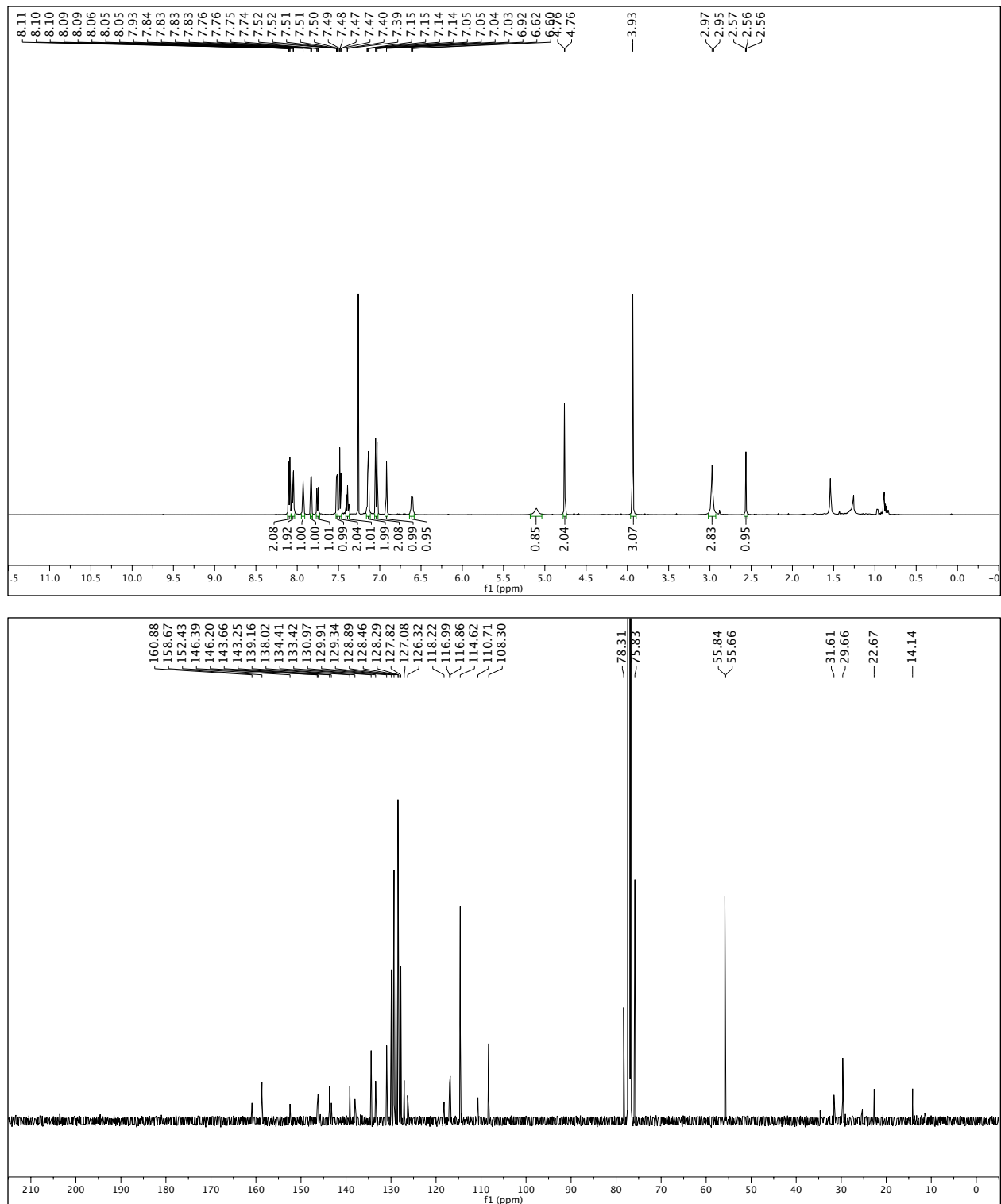
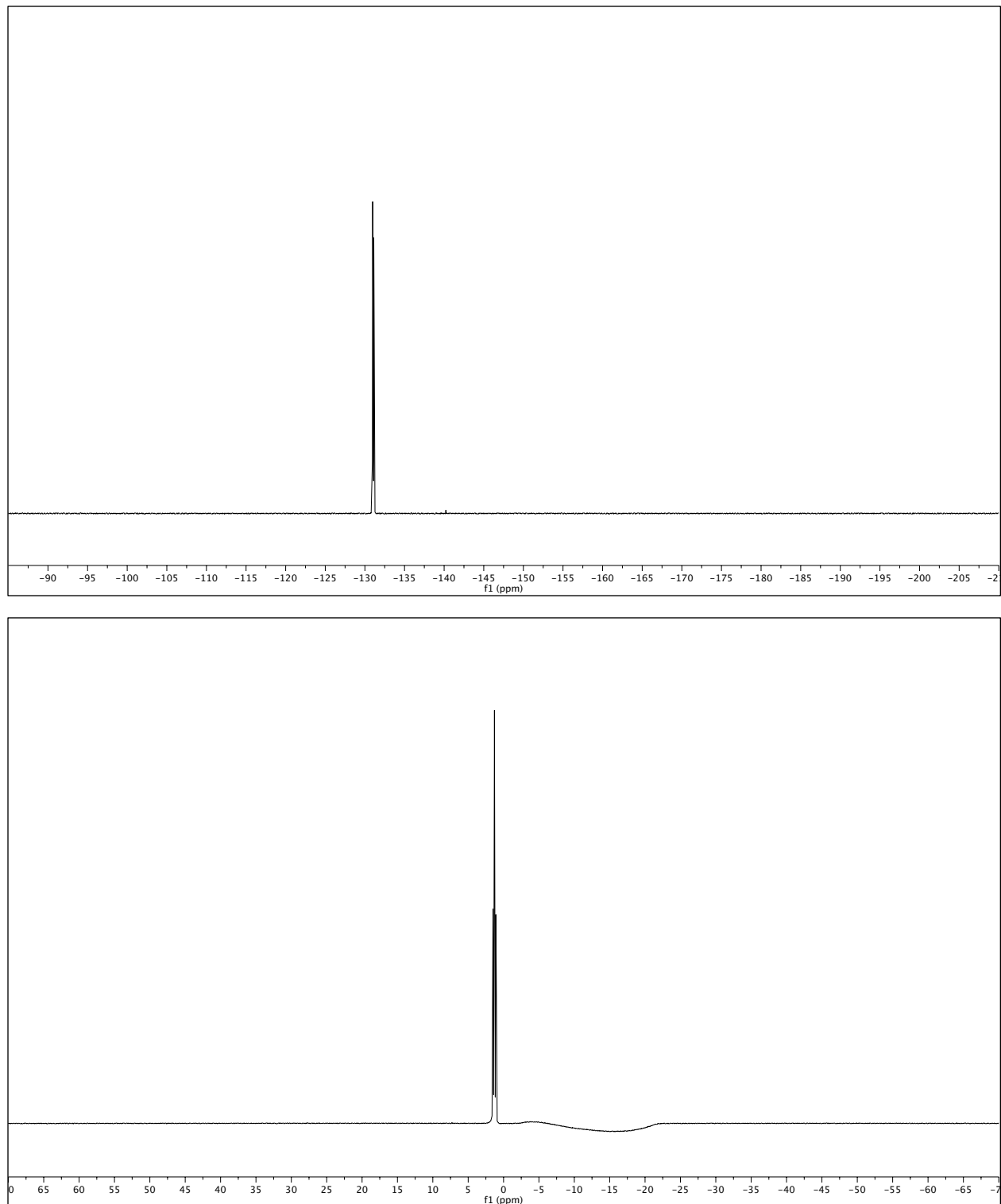


Figure S28.  $^1\text{H}$  NMR (500 MHz,  $\text{CDCl}_3$ ) and  $^{13}\text{C}$  NMR (125 MHz,  $\text{CDCl}_3$ ) spectra of compound 12.



**Figure S29.**  $^{19}\text{F}$  NMR (471 MHz,  $\text{CDCl}_3$ ) and  $^{11}\text{B}$  NMR (161 MHz,  $\text{CDCl}_3$ ) spectra of compound **12**.

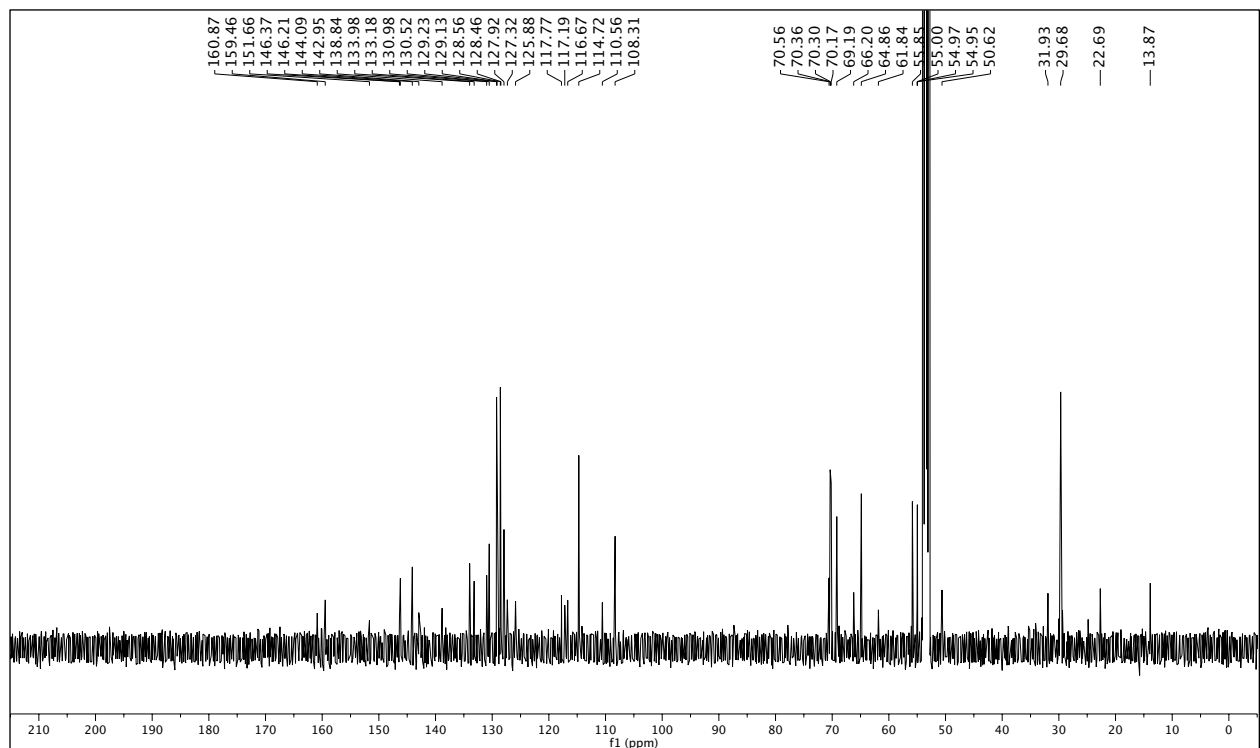
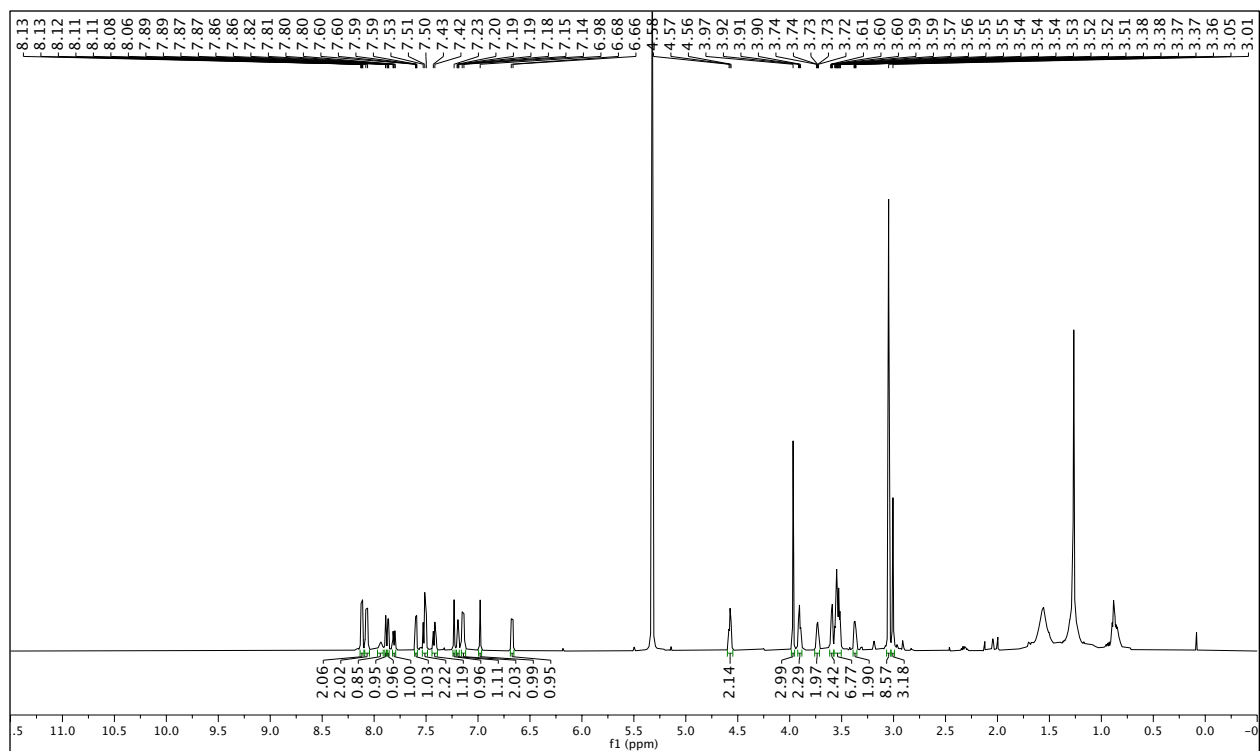
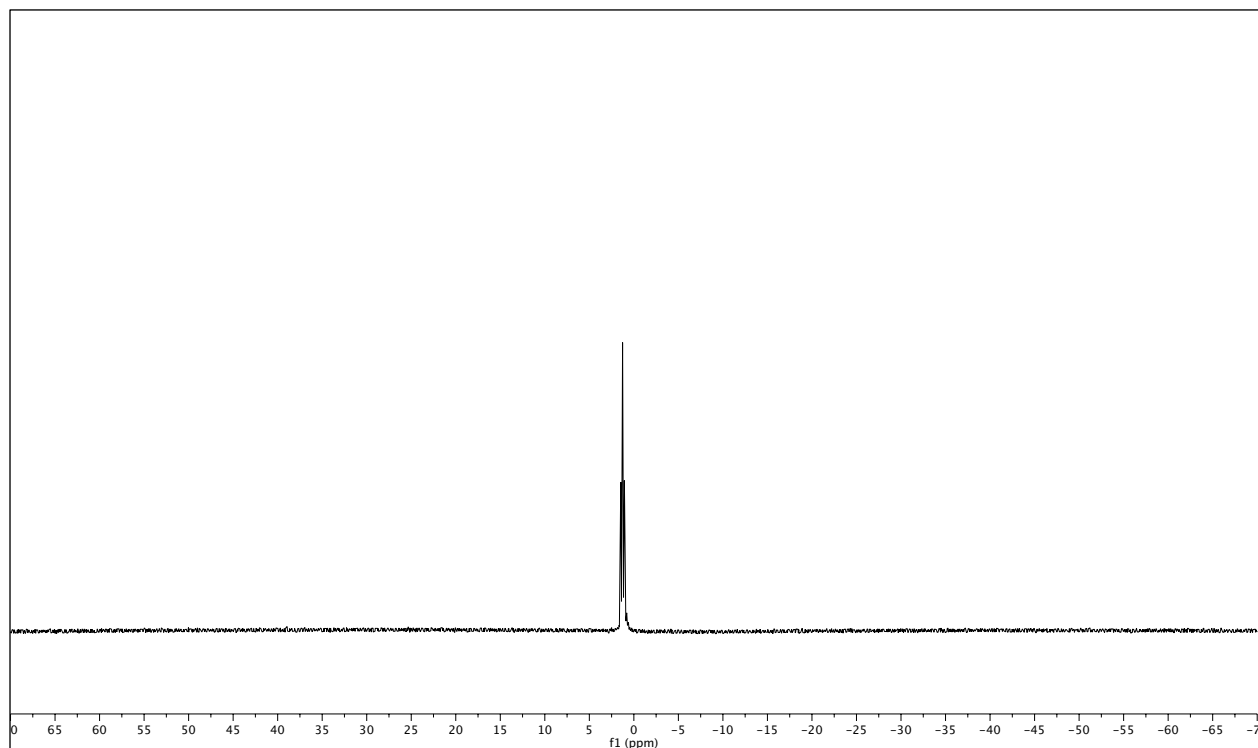
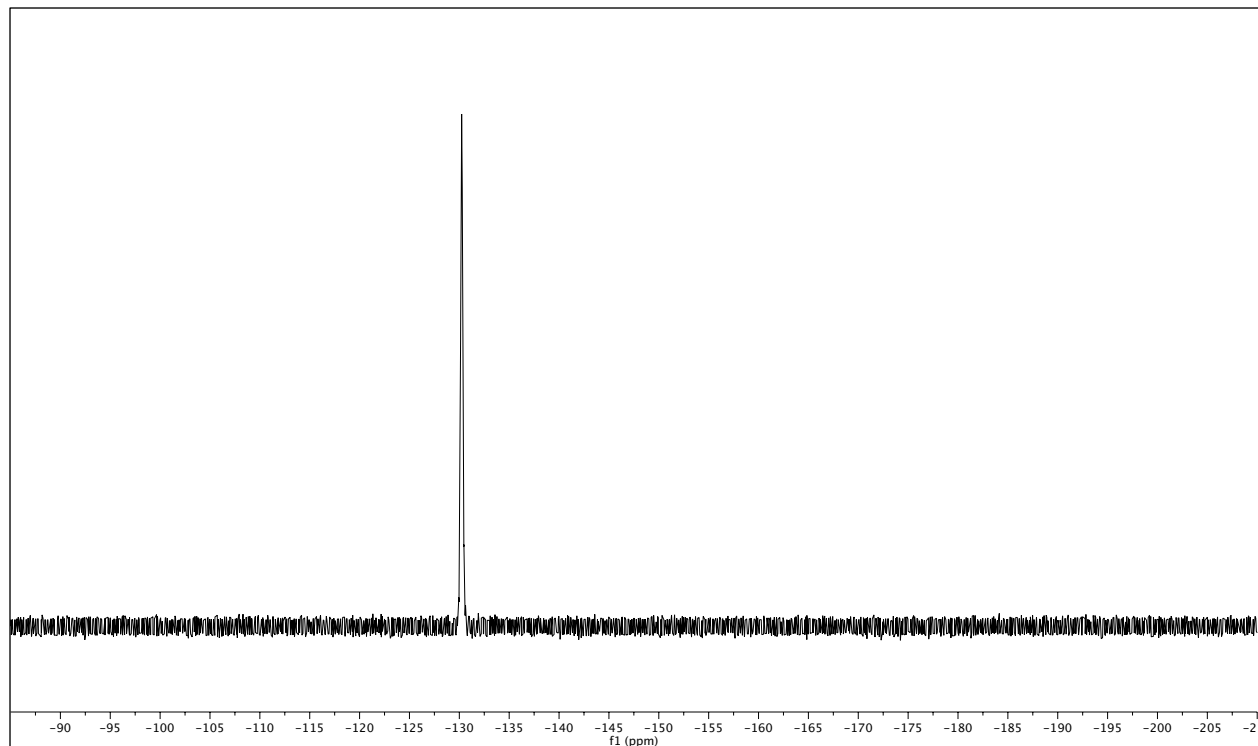
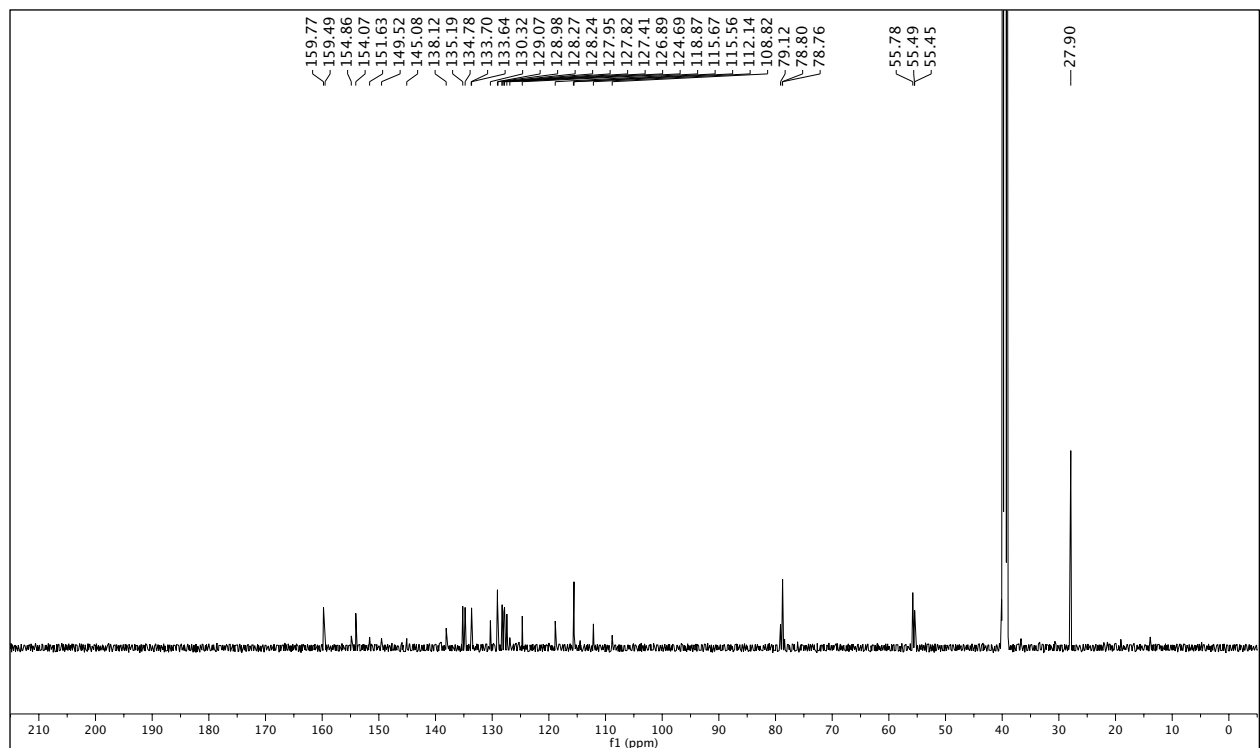
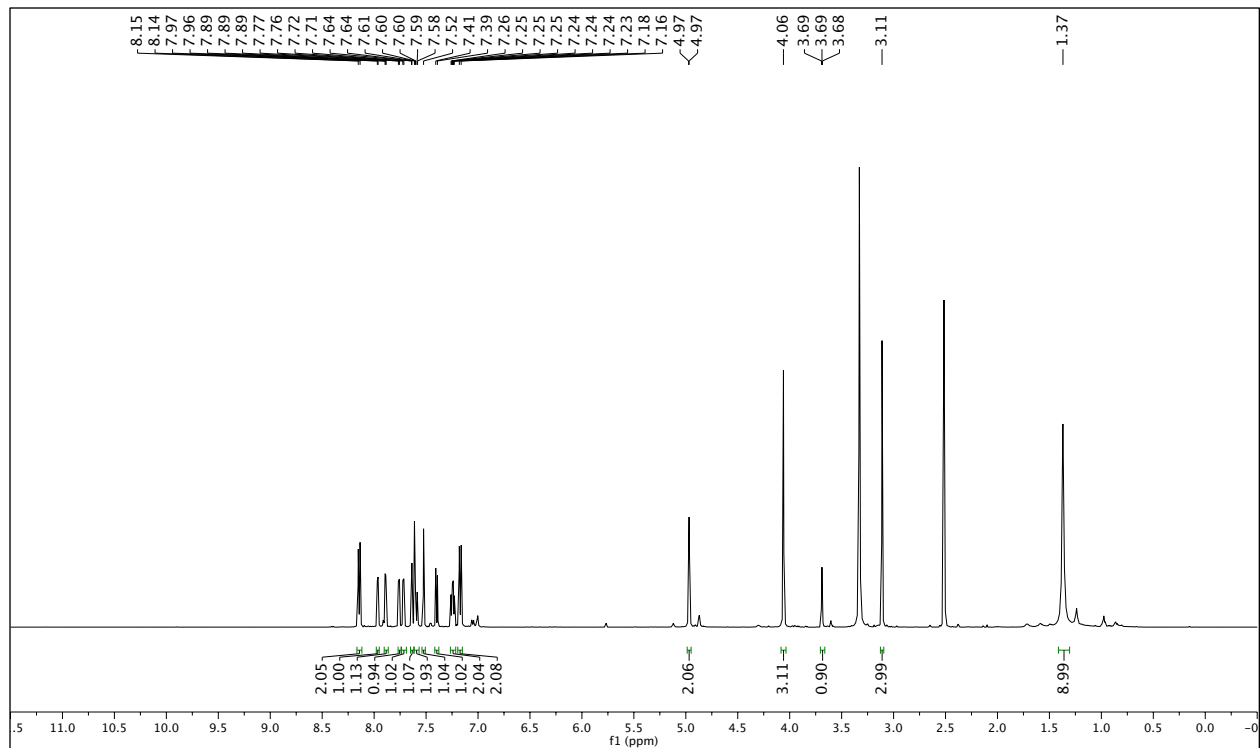


Figure S30.  $^1\text{H}$  NMR (500 MHz,  $\text{CD}_2\text{Cl}_2$ ) and  $^{13}\text{C}$  NMR (125 MHz,  $\text{CD}_2\text{Cl}_2$ ) spectra of **SR-APNO-2**.



**Figure S31.**  $^{19}\text{F}$  NMR (471 MHz,  $\text{CD}_2\text{Cl}_2$ ) and  $^{11}\text{B}$  NMR (161 MHz,  $\text{CD}_2\text{Cl}_2$ ) spectra of **SR-APNO-2**.



**Figure S32.** <sup>1</sup>H NMR (500 MHz, DMSO-*d*<sub>6</sub>) and <sup>13</sup>C NMR (125 MHz, DMSO-*d*<sub>6</sub>) spectra of compound **13**.

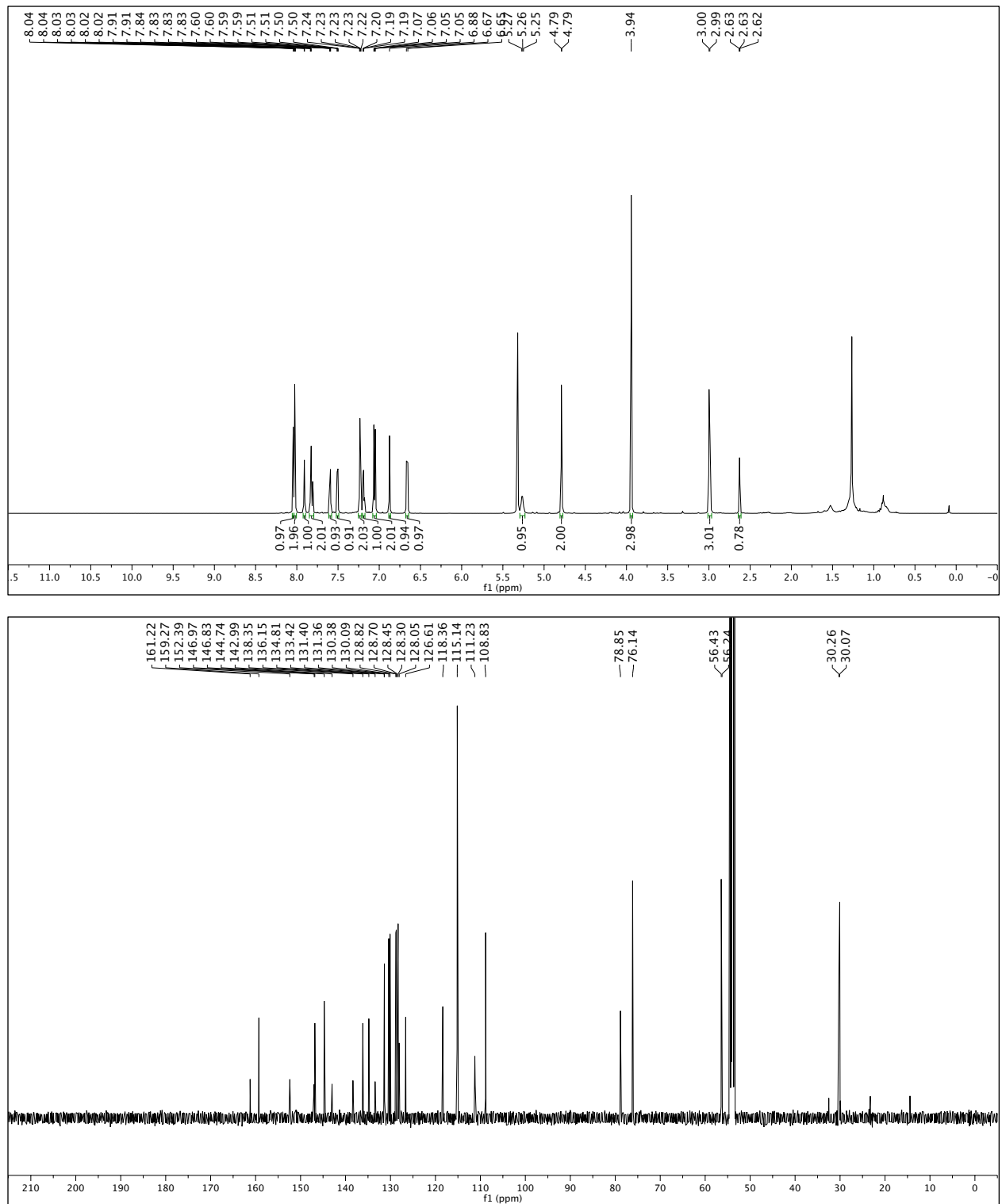
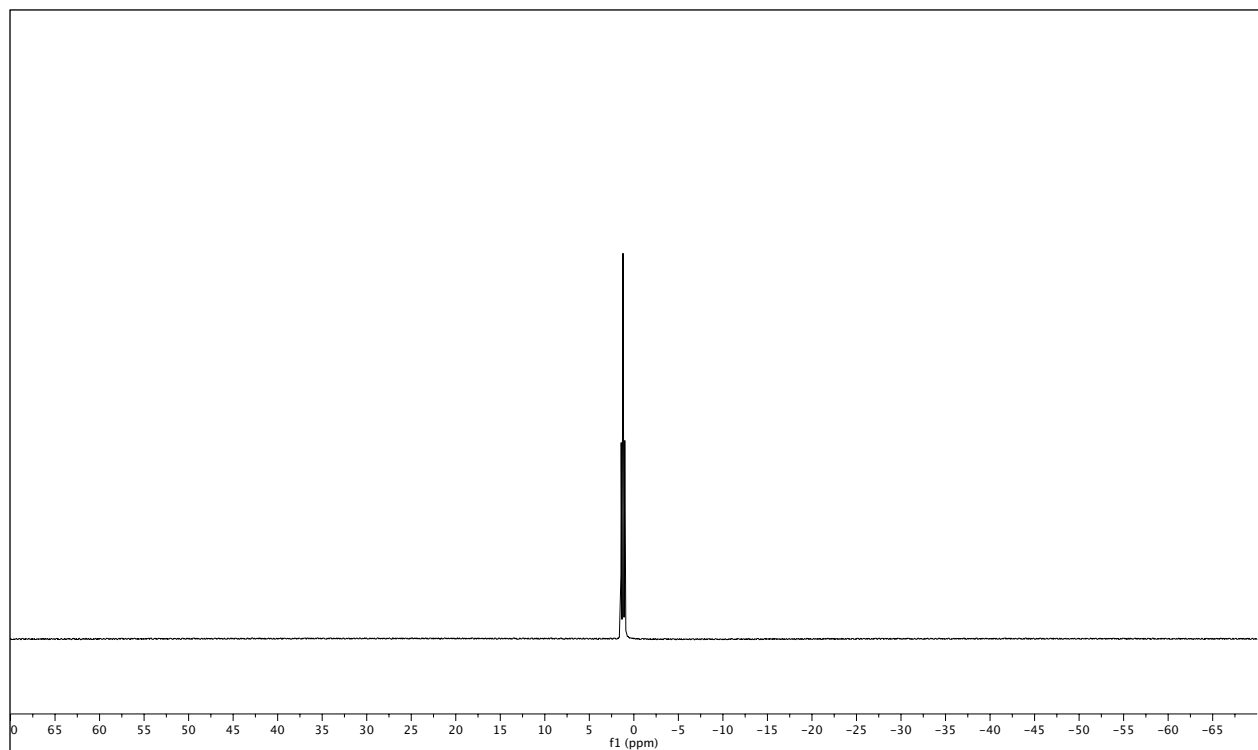
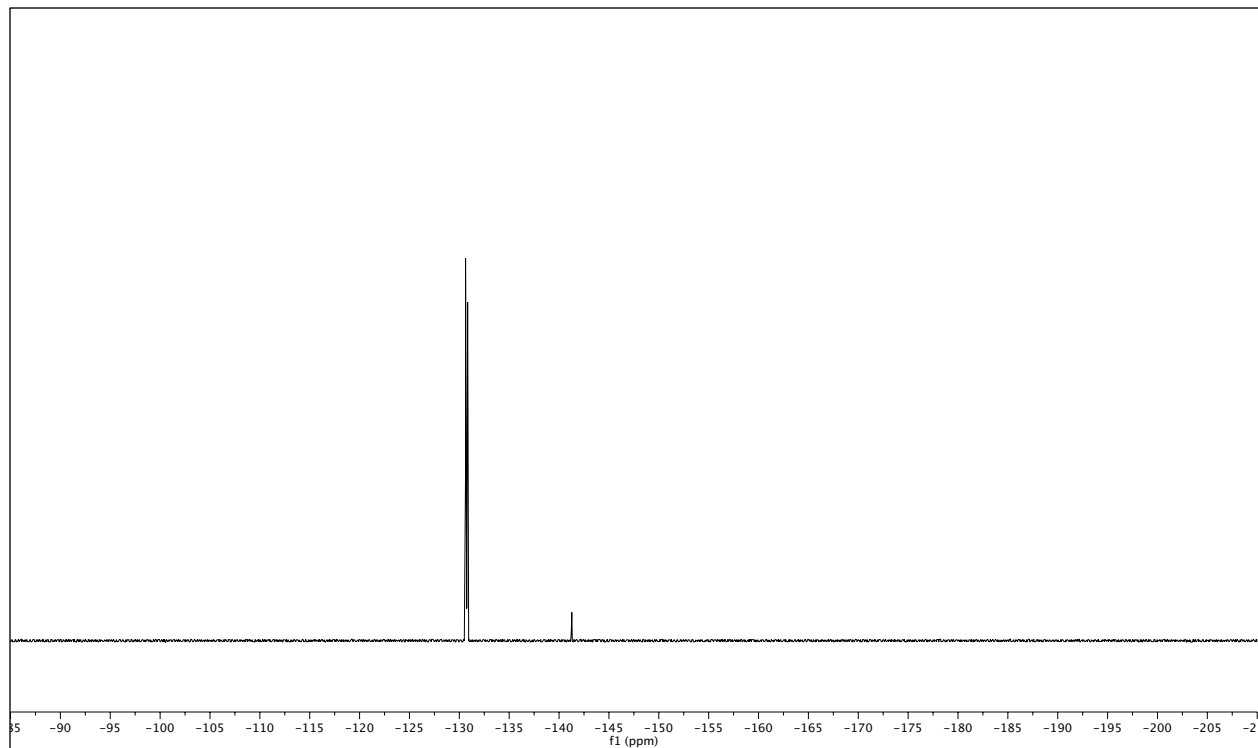


Figure S33.  $^1\text{H}$  NMR (500 MHz,  $\text{CD}_2\text{Cl}_2$ ) and  $^{13}\text{C}$  NMR (125 MHz,  $\text{CD}_2\text{Cl}_2$ ) spectra of compound 14.



**Figure S34.**  $^{19}\text{F}$  NMR (471 MHz,  $\text{CD}_2\text{Cl}_2$ ) and  $^{11}\text{B}$  NMR (161 MHz,  $\text{CD}_2\text{Cl}_2$ ) spectra of compound **14**.

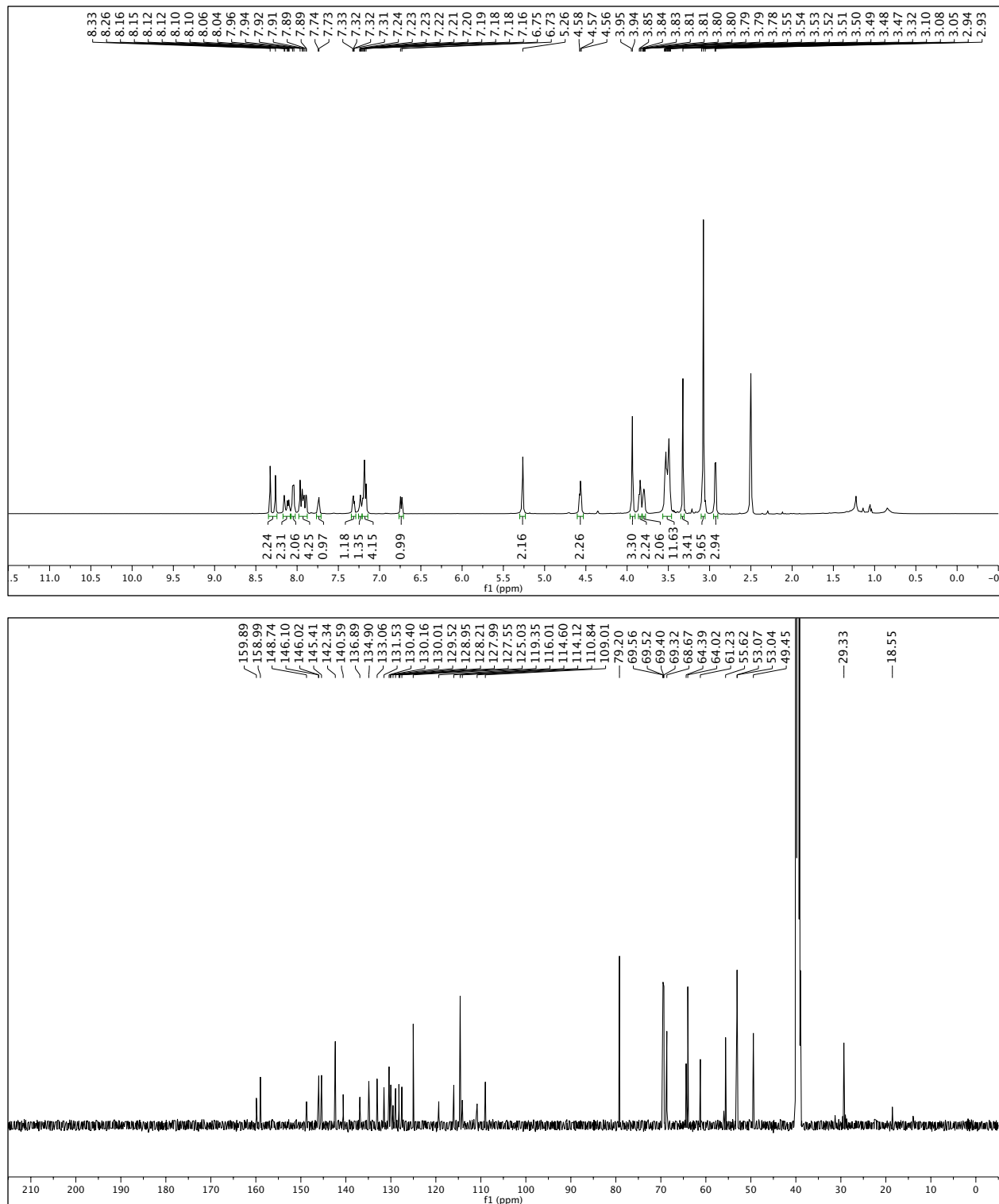
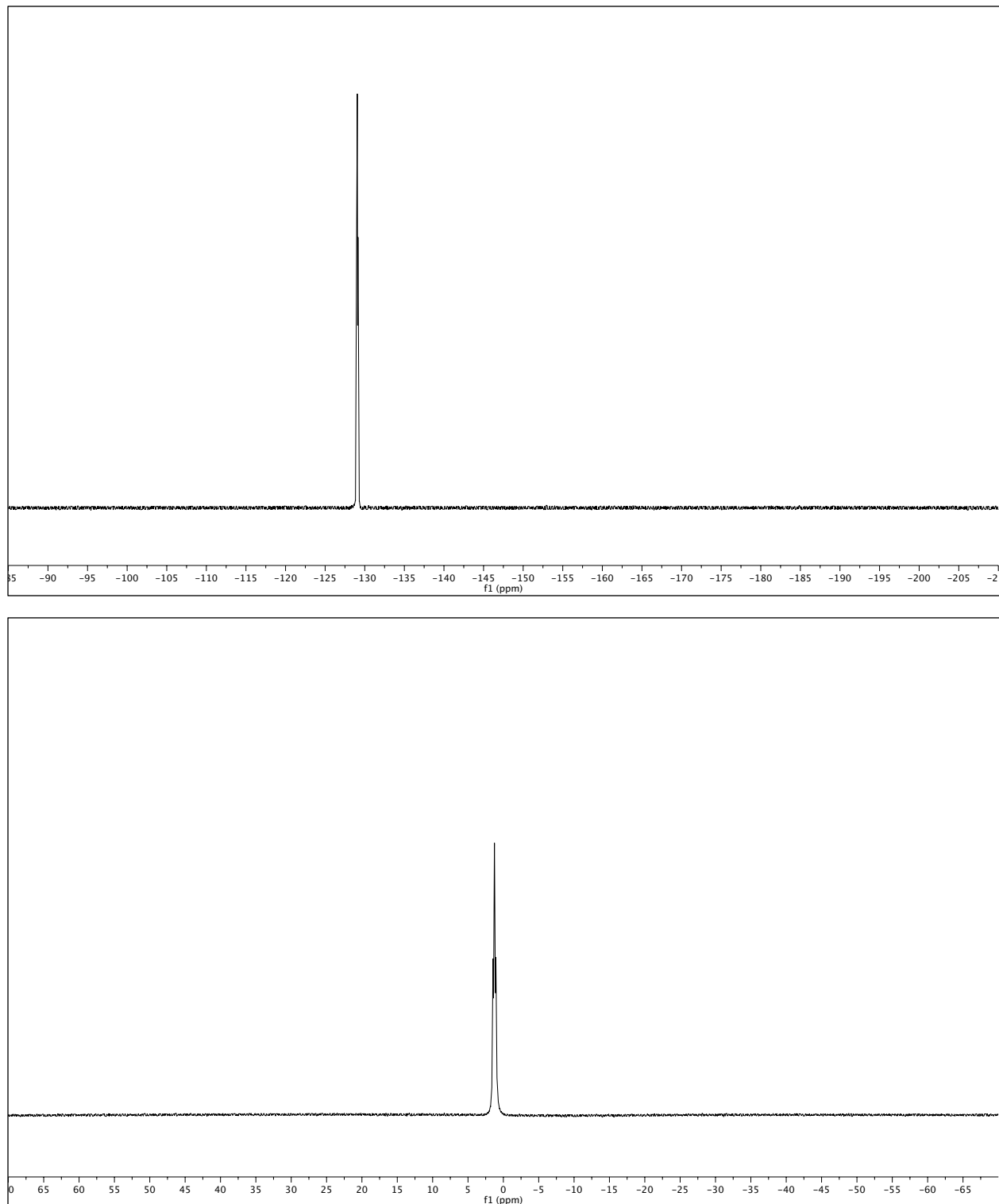


Figure S35. <sup>1</sup>H NMR (500 MHz, DMSO-*d*<sub>6</sub>) and <sup>13</sup>C NMR (125 MHz, DMSO-*d*<sub>6</sub>) spectra of SR-APNO-3.



**Figure S36.**  $^{19}\text{F}$  NMR (471 MHz,  $\text{DMSO}-d_6$ ) and  $^{11}\text{B}$  NMR (161 MHz,  $\text{DMSO}-d_6$ ) spectra of **SR-APNO-3**.

## Works Cited.

- 1 M. G. Suryaraman and A. Viswanathan, *J. Chem. Educ.*, 1949, **26**, 594.
- 2 M. D. Hanwell, D. E. Curtis, D. C. Lonie, T. Vandermeersch, E. Zurek and G. R. Hutchison, *J. Cheminform.*, 2012, **4**, 17.
- 3 A. K. Rappé, C. J. Casewit, K. S. Colwell, W. A. Goddard and W. M. Skiff, *J. Am. Chem. Soc.*, 1992, **114**, 10024–10035.
- 4 A. D. Becke, *J. Chem. Phys.*, 1993, **98**, 1372–1377.
- 5 P. J. Stephens, F. J. Devlin, C. F. Chabalowski and M. J. Frisch, *J. Phys. Chem.*, 1994, **98**, 11623–11627.
- 6 E. F. Pettersen, T. D. Goddard, C. C. Huang, G. S. Couch, D. M. Greenblatt, E. C. Meng and T. E. Ferrin, *J. Comput. Chem.*, 2004, **25**, 1605–1612.
- 7 T. Yanai, D. P. Tew and N. C. Handy, *Chem. Phys. Lett.*, 2004, **393**, 51–57.
- 8 C. Würth, M. Grabolle, J. Pauli, M. Spieles and U. Resch-Genger, *Nat. Protoc.*, 2013, **8**, 1535–1550.
- 9 W. Zhao and E. M. Carreira, *Angew. Chemie - Int. Ed.*, 2005, **44**, 1677–1679.
- 10 C. J. Reinhardt, E. Y. Zhou, M. D. Jorgensen, G. Partipilo and J. Chan, *J. Am. Chem. Soc.*, 2018, **140**, 1011–1018.
- 11 R. M. Uppu, *Anal. Biochem.*, 2006, **354**, 165–168.
- 12 A. Faustino-Rocha, P. A. Oliveira, J. Pinho-Oliveira, C. Teixeira-Guedes, R. Soares-Maia, R. G. Da Costa, B. Colaço, M. J. Pires, J. Colaço, R. Ferreira and M. Ginja, *Lab Anim. (NY)*, 2013, **42**, 217–224.
- 13 M. Liacha, S. Yous, J. H. Poupaert, P. Depreux and H. Aichaoui, *Monatsh. Chem.*, 1999, **130**, 1393–1397.
- 14 Q. Bellier, F. Dalier, E. Jeanneau, O. Maury and C. Andraud, *New J. Chem.*, 2012, **36**, 768.
- 15 X. Zhang, H. Yu and Y. Xiao, *J. Org. Chem.*, 2012, **77**, 669–673.
- 16 C. A. DeForest and D. A. Tirrell, *Nat. Mater.*, 2015, **14**, 523–531.
- 17 H. T. S. Britton and A. R. Robinson, *J. Chem. Soc.*, 1931, **0**, 1456–1462.
- 18 C. Amatore, S. Arbault, C. Ducrocq, S. Hu and I. Tapsoba, *ChemMedChem*, 2007, **2**, 898–903.